IGCP project 683: Pre-Atlantic Geological Conections among Northwest Africa, Iberia and Eastern North America: Implications for Continental Configurations and Economic Resources

Guide to the Iberian Field Trip (May 8th-13th, 2023)

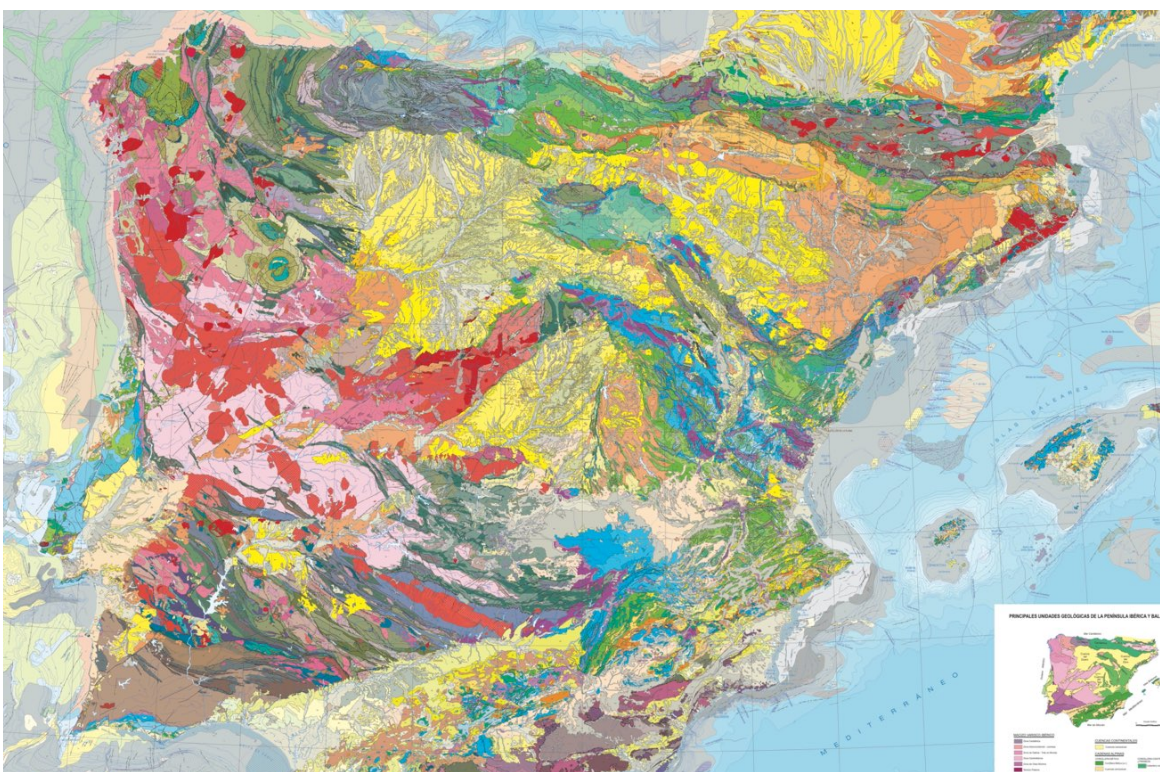

Authors:
Central Iberian Zone: F. Bea, A. Cambeses, P. Montero, JF. Molina, L. Barcos
Ossa-Morena Zone: A. Azor, D. Poyatos, J.F. Simancas, I. Pérez-Cáceres, I. Expósito Ramos, C. Accotto.
South Portuguese Zone: J. de la Rosa, T. Donaire

Foreword

Welcome to the geological field trip in the Iberian Massif! During this field trip, we will have the opportunity to explore this region's rich and complex geology. We will also have the opportunity to experience the culture and history of central-south Spain with visits to local villages and historic sites. After a general description of the Iberian Massif, we intended to describe the route and the outcrops we shall visit. Readers must understand that it is neither a research paper nor an exhaustive summary of the current knowledge, simply a field trip guide inevitably slanted according to the authors' opinions and prejudices, the major of which was to emphasize preferentially the description of the three zones that we shall visit, Central Iberia, Ossa Morena and South Portuguese. To keep it simple and readable during field visits, we included just a few inescapable references in the text; instead, we gave a list of valuable lectures and seminal papers at the end of the guide.

Introduction

Most of the pre-Mesozoic basement of Central and Western Europe consists of Neoproterozoic and Palaeozoic rocks that were deformed, locally metamorphosed until anatexis, and intruded by Carboniferous granitoids during the Variscan orogeny. These materials form the West-European Variscan Belt, resulting from the collision of two main continental masses, Laurussia and Gondwana, that also involved some minor continental masses, such as Avalonia or Armorica.

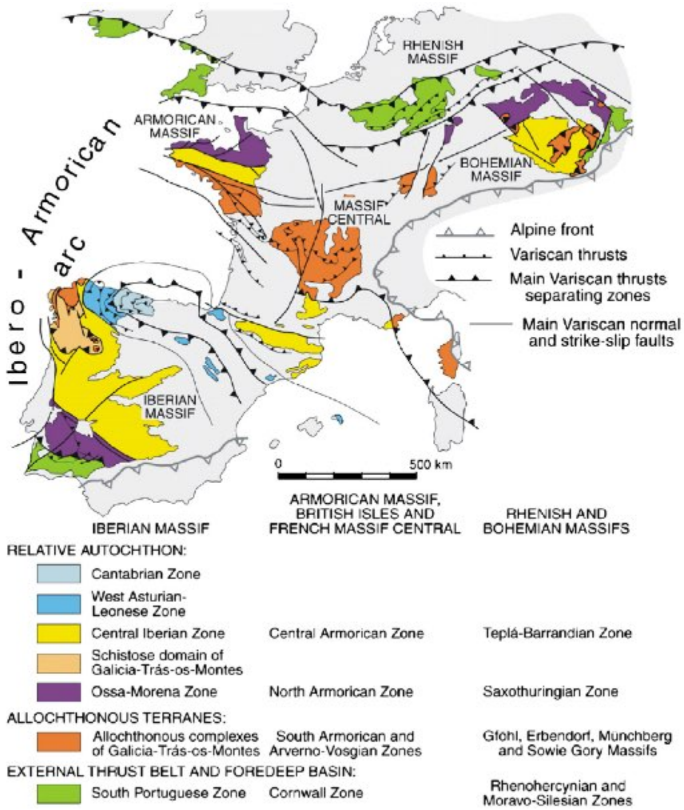

Figure 1.- The west European Variscan Belt (from Murphy et al. 2010)

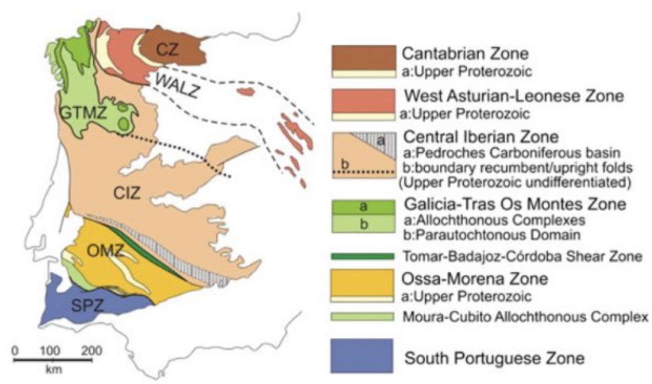

Figure 2.- Zonal division of the Iberian Massif (from Simancas, 2019)

The largest outcrop of the West European Variscan Belt occurs in the Iberian Peninsula, occupying most of Portugal and West Spain (Fig. 1). It is indistinctly called Iberian Massif, Hesperian Massif, or Hercynian Massif, although the first variant is the most frequently used.

The Iberian Massif contains autochthonous and allochthonous Paleozoic and Neoproterozoic materials structured as an S-shaped oroclinal belt with a well-defined convex-to-the-west arc centred in Asturias and a poorly defined convex-to-the-east arc centred in central Iberia (Fig. 2).

The Asturian Arc (also known as the Asturian Knee) continues to the French Armorican Massif forming the Ibero-Armorican Arc (Fig. 1). The Asturian and Armorican Arcs were separated during the Mesozoic opening of the Biscay Gulf.

Since Lotze (1945), the Iberian Massif has been divided into several, classically six, zones according to their stratigraphic, tectonic, metamorphic and magmatic features. From NNE to SSW, the Lotze zones, slightly modified by later authors (e.g., Julivert et al., 1974) are the following: Cantabrian (CZ), West-Asturian Leonese (WALZ), Central Iberian (CIZ), Galicia Tras-os-Montes (GTMZ), Ossa Morena (OMZ) and South Portuguese (SPZ) (Fig. 2). The Cantabrian and South Portuguese Zones are the most external zones, containing syn-orogenic and post-orogenic sediments, with no, or very low, degree of metamorphism and thin-skin tectonics that caused folds and nappes with opposite vergence, to the E in the Cantabrian and West-Asturian Leonese zones and the WSW in the South Portuguese zone. The intensity of metamorphism and deformation increase towards the most internal zones, so about 50% of the Central Iberia crust consists of Variscan granitoids which, remarkably, do not show across-orogen polarity.

Although most authors agree *grosso modo* with this division, Arenas et al. (2016) have proposed to join the GTMZ and the OMZ in one single allochthonous zone, the Galicia-Ossa-Morena Zone, but this idea has not been unanimously accepted.

Zones of the Iberian Massif

1. Cantabrian Zone (CZ)

The Cantabrian Zone (Fig. 3) is the external zone of the Iberian Massif in the NW of the Peninsula, placed in the core of the Ibero-Armorican Arc. It contains mainly Palaeozoic sedimentary rocks, from Cambrian to Upper Carboniferous. Neoproterozoic sedimentary rocks are restricted to the Narcea Antiform, located to the west in the boundary with the West-Asturian Leonese Zone marking the transition to the internal zones of the orogen.

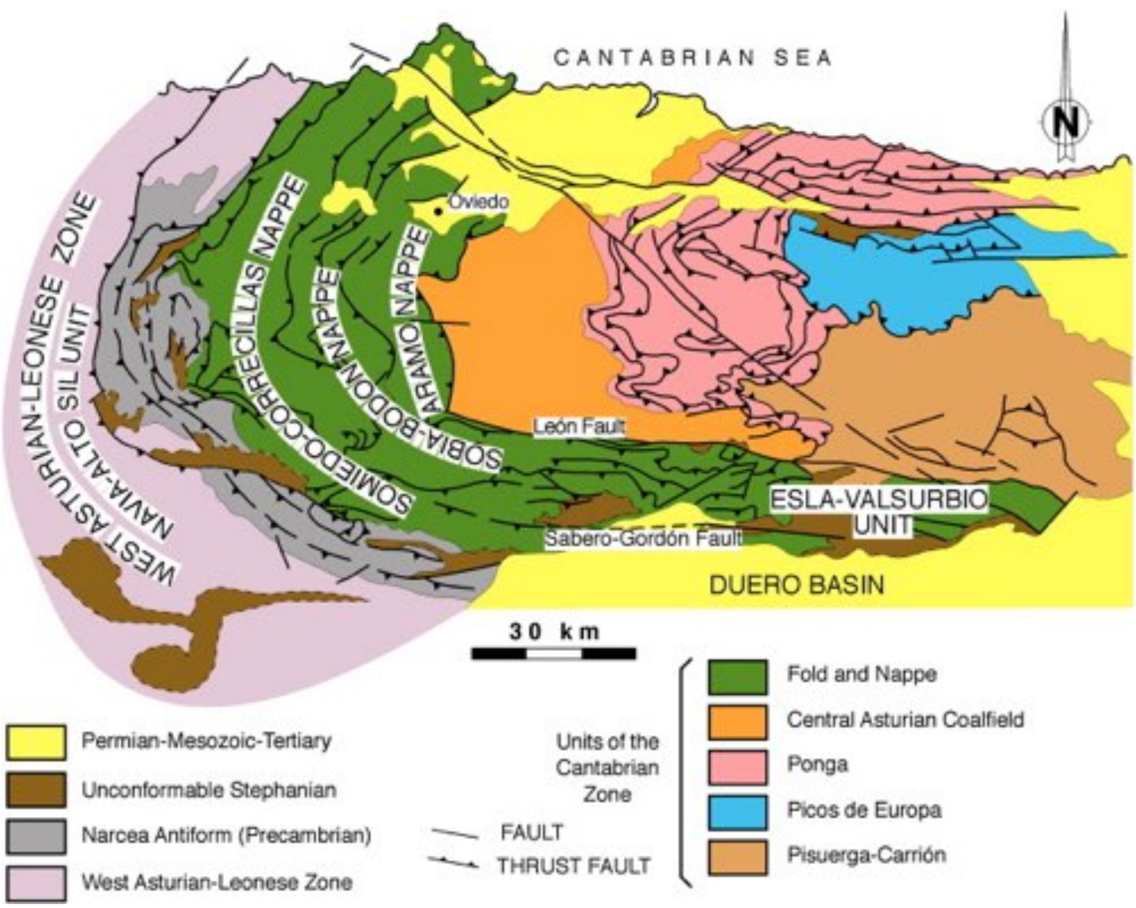

Fig.3.- Cantabrian Zone, based on Julivert, 1971.

The pre-Stephanian series, discordant over the Neoproterozoic rocks, has been divided into pre-orogenic and syn-orogenic, the limit between them roughly situated at the Devonian-Carboniferous boundary. The pre-orogenic rocks form a shallow marine sequence thinning to the east. The syn-orogenic deposits are mainly clastic and siliciclastic with interbedded exploitable coal layers and massive limestones, especially in the east. Post-orogenic Stephanian sedimentary rocks appear locally, always discordant on the earliest Carboniferous materials.

The tectonic is thin-skinned, with abundant recumbent folds and nappes. The metamorphism is very low (anchimetamorphism) or absent, with no —or very local— schistosity development. There are some pre-Variscan volcanic rocks, chiefly alkali basalts and trachybasalts, and a few small Variscan plutons and dykes, which may be associated with small gold deposits.

2. West-Asturian Leonese Zone (WALZ)

It is a 100 km wide curved band that follows the Ibero-Armorican Arc (Fig. 4) limiting with the Cantabrian Zone through La Espina Thrust, placed in the core of the Narcea Antiform. In contrast with the Cantabrian Zone, dominated by non-schistose upper Paleozoic sedimentary rocks, the West-Asturian Leonese zone mostly consists of schistose Cambrian to Ordovician low-grade metasediments that form a thick (>= 11,000 m) siliciclastic series with alternating minor volcanoclastic and limestone levels. Also contrasting with the Cantabrian zone, the rocks in this area show generalized tectonic foliations and marked internal strain.

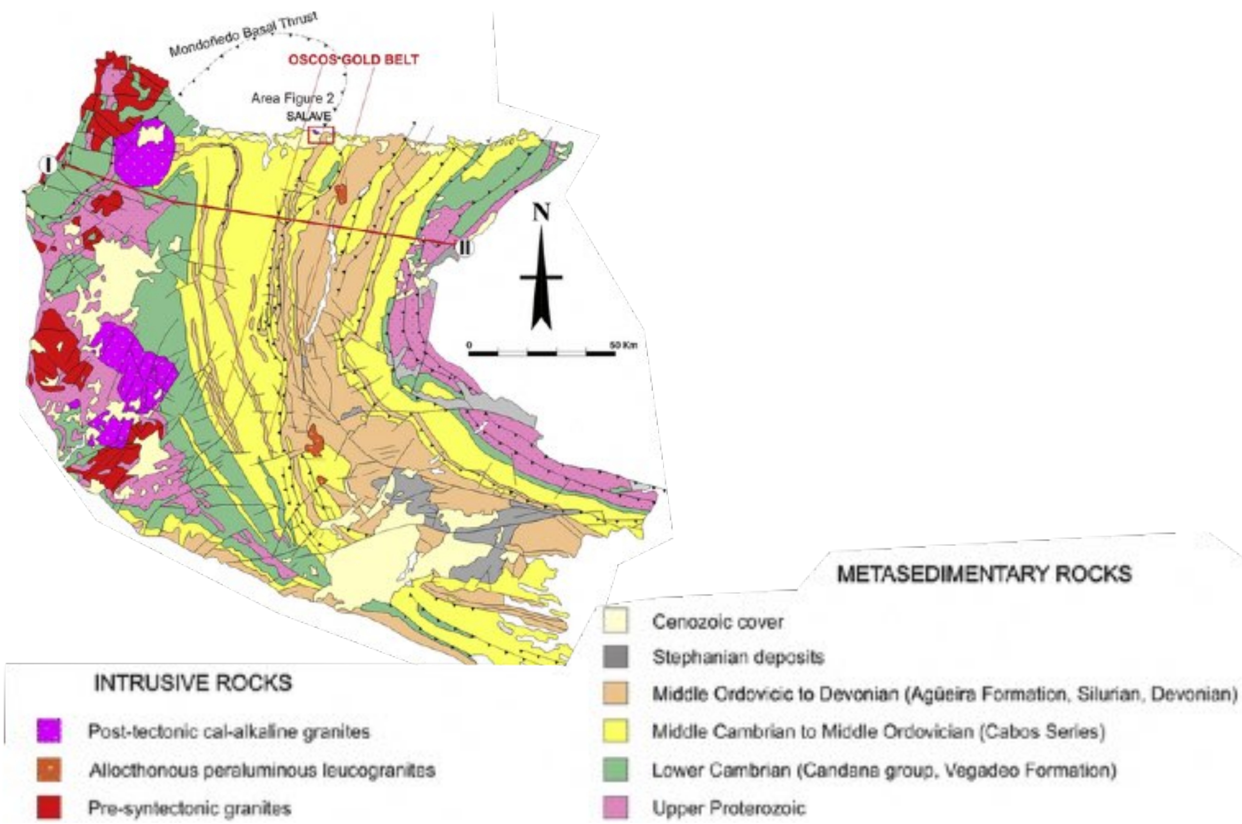

Fig.4.- West-Asturian Leonese Zone, from Pérez-Estaún et al., 1990

Based on the stratigraphic differences, most authors consider this zone divided into two domains: (i) the Navia and Alto Sil Domain and (ii) the Manto de Mondoñedo Domain.

Structurally, the WALZ is characterized by folds with axial plane vergent to the east, more flattened and tighter to the west, cut by thrusts vergent to the same direction and subsequently folded with vertical axes. The metamorphism is low to medium grade, more intense towards the west. It is of low grade in the Navia and Alto Sil Domain but may be of high grade in the Manto de Mondoñedo Domain.

The increase of metamorphic grade towards the internal zones of the orogen is accompanied by the intrusion of granite plutons, commonly composed of peraluminous granites to granodiorites, which may be associated and hybridized with mafic rocks. These granite rocks match the ones found in the Central Iberian Zone, described below.

3. Central Iberian Zone (CIZ)

It is the widest (about 350 km) zone of the Iberian Massif and includes the axial part of the Variscan orogen (Fig. 5). The Vivero fault bounds it to the NE and the Badajoz-Córdoba shear zone to the SSW. It contains all autochthonous materials underneath the Basal Thrusts of the Schistose Domain of the Galicia Tras-os-Montes Zone (see below).

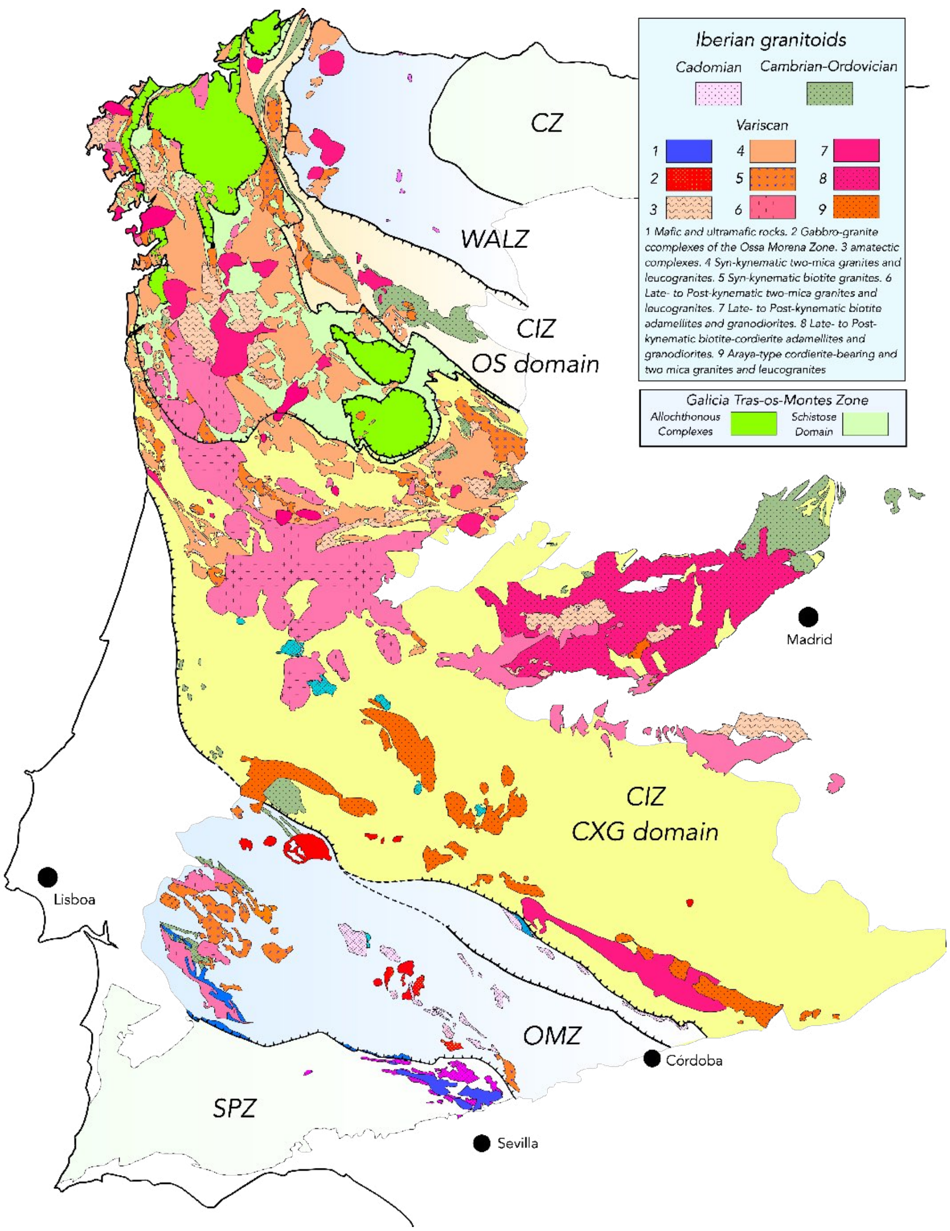

Figure 5. Central Iberian and Galicia Tras-os-Montes Zones, with the representation of granitoid bodies found all over the Iberian Massif.

Stratigraphically, it stands out for the transgressive nature of the Lower Ordovician quartzites and the predominance of pre-Ordovician rocks, according to the nature of which most authors divide the Central Iberian Zone into two large domains parallel to the zone boundaries, the smaller Ollo de Sapo Domain (OSD) in the north, and the larger Schist-Greywacke Complex Domain (SGCD), in the south.

The Ollo de Sapo (Toad's Eye) Formation consists of porphyritic, all most often augen, gneisses of granite to granodiorite composition derived from Cambrian-Ordovician (c.a. 490 to 475 Ma, Montero et al., 2009) volcanic and plutonic rocks; it appears in antiform cores and crops out forming a narrow band about 600 km long. The rock is characterized by large K-feldspar augen, locally rapakivi, and small bluish quartz clasts, the colour of which disappears with increasing metamorphic grade.

The Schist-Greywacke Complex is a thick monotonous series of metapelites and metapsamites with no fossil record and Ediacaran to Lower Cambrian age which crops out in wide antiforms of Portugal and West Spain.

The pre-Variscan tectonics is only evident in the SGC Domain because of three discordances, two intra-Ediacaran and the other in the Lower-Medium Cambrian. The Variscan tectonics caused three main deformation phases. The first deformation phase, Late Devonian to Early Carboniferous, caused the major structures to thicken the Central Iberian crust. In the Ollo de Sapo Domain, these structures consisted of recumbent folds and nappes that were later re-folded and verticalized during the third phase. The second phase was local, related to low-angle thrust faults in higher structural domains and granite intrusion and subhorizontal shear zones in the deeper structural domains. The first phase was also intense tangential in the NE and SW borders of the Schist-Graywacke Domain. It, however, produced vertical folds in the central areas. The second phase, particularly intense in thermal domes, yielded subhorizontal shear zones. The third phase tightened the previous structures and caused different systems of conjugated vertical shear zones.

The pre-Variscan magmatism in Central Iberia occurred during the Ediacaran and the Cambrian-Ordovician. The Ediacaran magmatism should have been particularly intense, as revealed by the abundance of c.a. 590-620 Ma detrital zircons in the Schist-Graywacke Complex and inherited zircon cores in the Ollo de Sapo gneisses. Few of these rocks, however, were preserved; their current occurrence is limited to the small c.a. 580 Ma gabbro-dioritic massif of Merida-Aljucén and the singular c.a. 543 Ma of La Almohalla (Bea et al., 2003).

The Cambrian-Ordovician magmatism is represented by (i) the Ollo de Sapo Formation gneisses in the NE border, (ii) the similar Urra Formation gneisses in the SW border (Solá et al., 2008), (iii) a band of medium-sized undeformed leucotonalites and high-silica granites in the centre roughly following the Variscan structures (Rubio-Ordónez et al., 2012). A remarkable feature of the Ollo de Sapo and the Urra gneisses is the elevated zircon inheritance; in most cases, nearly 90% of zircon grains are composed of an Ediacaran core surrounded by a Cambrian-Ordovician rim (Bea et al., 2007). In contrast, the central band undeformed Cambrian-Ordovician granitoids have zircons with very little or no inheritance.

The Variscan magmatism caused numerous granite batholiths ranging from allochthonous to autochthonous, related to thermal domes and anatectic complexes. These granites are crustal, derived from the Cambrian-Ordovician gneisses and fertile layers of the Schist-Grauwacke Complex, with few juvenile mantle-derived components. These are represented by small plutons and stocks of mafic rocks, mostly appinites and vaugnerites that are coeval or slightly postdate the related granites (Bea et al., 2021). The age of these falls within a narrow range of 315 ± 15 Ma, independent of their position relative to the orogenic axis (Bea et al., 2003).

4. Galicia Tras-os-Montes Zone (GTMZ)

The Galicia Tras-os-Montes Zone (Fig. 5) consists of allochthonous and para-autochtonous terranes emplaced over the Central Iberian zone's northern part. It comprises two stacked domains, the lower Schistose Domain and the upper Allochthonous Complexes Domain.

The Schistose domain is made of siliciclastic metasediments and metavolcanic rocks, which, although not identical, bear similarities with those found in the Central Iberian Zone. Accordingly, it is assumed that both formed on the same continental margin of Gondwana but in different positions.

The Allochthonous Complexes Domain comprises four roughly oval large mafic-ultramafic complexes: Cabo Ortegal, Ordenes, Morais and Braganza, and one N-S elongated zone, the Blastomilonitic Fossa, composed of felsic, often peralkaline, granites and volcanic rocks. The materials forming these allochthonous complexes are uncommon in the rest of the Iberian Massif. They include ophiolites and mixed materials of continental and, possibly, island arc origin. The provenance of these exotic items is uncertain.

5. Ossa Morena Zone (OMZ)

The OMZ forms a ca. 90 km wide NW-SE band (Fig. 6) that evidences a complex evolution during the late Neoproterozoic Cadomian orogeny, 650-550 Ma, Cambro-Ordovician, 540-480 Ma, and 370-300 Ma Carboniferous Variscan orogeny. It bounds north with the Central Iberian Zone through the Badajoz-Cordoba Shear Zone and south with the South Portuguese Zone through South Iberian Shear Zone. Along this boundary, there is a lineament of exotic units, namely the Moura-Cubito HP complex and the Beja-Acebuches amphibolites, which have been considered remnants of the Rheic Ocean. As we shall discuss during the field trip, there is considerable discussion about this aspect.

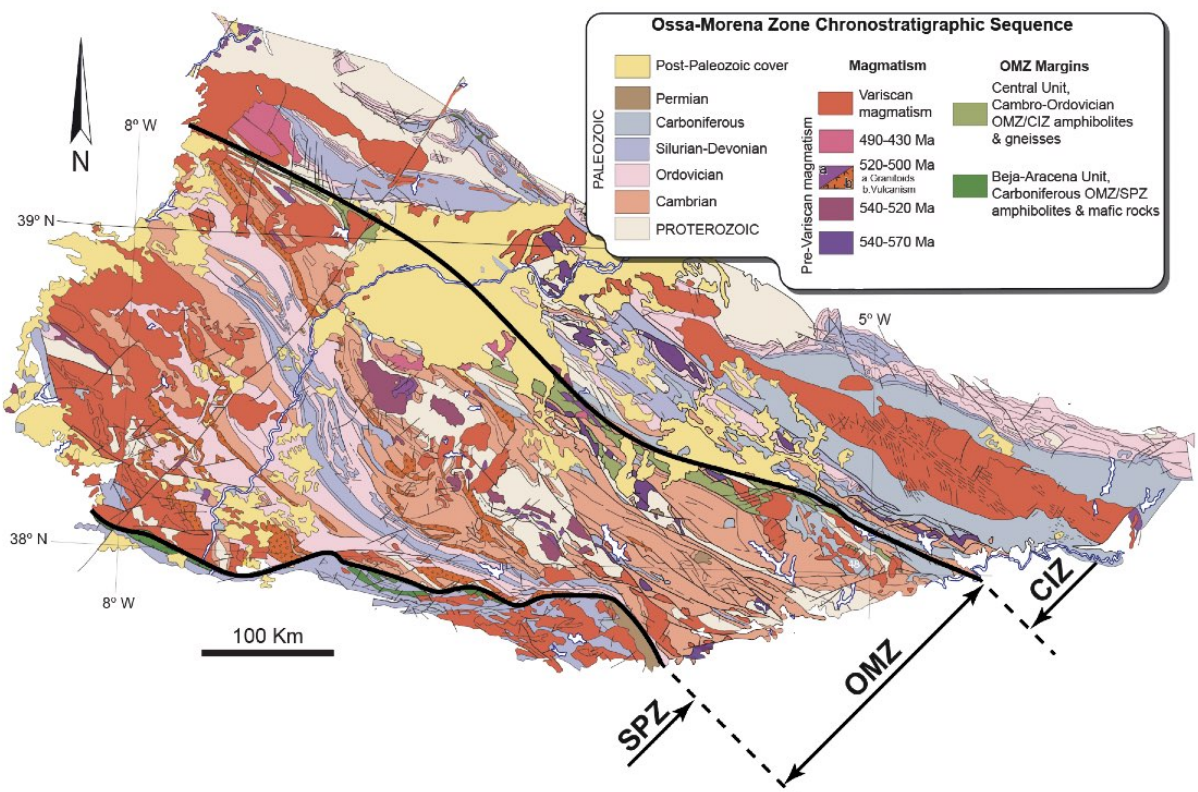

Figure 6. The Ossa Morena Zone. The coarse solid lines represents the Badajoz-Córdoba Shear Zone and Beja-Acebuches amphibolites, the boundaries with the Central Iberian Zone and South Portuguese Zone respectively. After Cambeses et al., (2017)

The OMZ stratigraphic succession includes Ediacaran to early Carboniferous rocks. The basement comprises the Ediacaran Serie Negra, consisting of black shales, quartzites and metagreywackes overlain by the Malcocinado Formation, composed of arc-related volcano-sedimentary successions. The contact with Cambrian sediments is unconformable contact associated with a stage of rifting. Ordovician is dominated by passive margin deposits. Overlying the Ordovician sediments is a monotonous series of Silurian black shales covered by Early Devonian shallow-water terrigenous series. The transition from Early to Middle-Late Devonian is marked by a discordance related to the beginning of the Variscan collision. Tournaisian-Visean turbidites mark the intra-orogenic extension.

The OMZ preserves structures related to various transpressional and transtensional events from the late Neoproterozoic to the early Carboniferous. Pre-Variscan structures were overprinted by the Variscan deformation producing the complex structural relationships that characterize the OMZ. The Variscan structures preserve evidence of an initial collisional event between 390–345 Ma that resulted in large recumbent southwest vergent folds, like the Olivenza-Monesterio antiform, and thrusts that cut the recumbent folds, like the Monesterio thrust. This was followed at 345–330 Ma by extension/transtension resulting in the Carboniferous basins formation. Finally, a second collisional event at 330–305 Ma generated vertical folds that deformed the previous structures. Post-Variscan high-angle reverse faults subsequently cut the upright folds.

The metamorphism that affected the OMZ was generally low-grade, although some areas record high-grade conditions. Among these, they stand up (i) the Pre-Variscan 532–500 Ma found in the Valuengo and Monesterio complexes, related to a Cambro-Ordovician rifting; (ii) the Variscan 390–370 Ma LT/HT-HP identified in the Badajoz–Cordoba shear zone and the Cubito-Moura unit; (iii) the late Variscan ca. 340–323 Ma HT-LP metamorphism in the Campo Maior–Arronches–Crato region and the Évora–Aracena–Lora del Rio metamorphic belt.

The OMZ magmatism can be divided into three main stages: Neoproterozoic-Cambrian Cadomian collision-related; Cambro-Ordovician, extension-related; and Carboniferous Variscan to Permian collision- and extension-related

The Neoproterozoic–Cambrian, 590–540 Ma, magmatism mainly comprises Cadomian arc diorites to granites and basalts, which are preserved as metabasite and amphibolites. The early rift-related Cambrian magmatism occurred between 540-520 Ma. It produced peraluminous to metaluminous and peralkaline A2-type granites during the initiation of extension. The main rift-related late Cambrian event at 520–500 Ma produced abundant bimodal plutonic and volcanic rocks. The mafic terms show a diachronic transition from E-MORB-like at 517-512 Ma to OIB-like at 512-505 Ma. The felsic terms consisted of anatectic peraluminous intermediate to felsic granitoids and peralkaline A-type granites. From 490 to 470 Ma, the Cambro-Ordovician rifting produced T- and N-MORB-like mafic rocks. Coeval felsic magmatism was also extension-related: peralkaline A1-type anorogenic and peraluminous anatectic.

The Carboniferous magmatism, 350-330 Ma, was a product of the Variscan Orogeny. It includes minor volcanism, interbedded in Carboniferous sediments, and extensive plutonism. The magmatism is spread throughout the OMZ in five main regions: i. the La Coronada-Villaviciosa complex, ii. the Nisa-Santa Eulalia plutons, iii. the Évora Massif, iv. the Beja-Aracena intrusive complex and v. the Olivenza-Monesterio complex. In all these regions, magmatism comprises ultrabasic to acid, alkaline to sub-alkaline tholeiitic and calc-alkaline plutons and peraluminous intrusions that may form complicated gabbro-granite intrusions such as Burguillos del Cerro. As discussed during the field trip, this magmatism seems to be related to the mid-crustal emplacement of multiple mafic sills revealed by the existence of a marked seismic reflector, the Iberseis Reflective Body (IRB). The last magmatic event in the region was Permian, c.a. 290 Ma, which caused the extension-related intrusion of dolerite dykes.

6. South Portuguese Zone (SPZ)

It is the South external region of the Iberian Massif, bounded to the north by the Ossa Morena Zone through the South Iberian Shear Zone (Fig. 7).

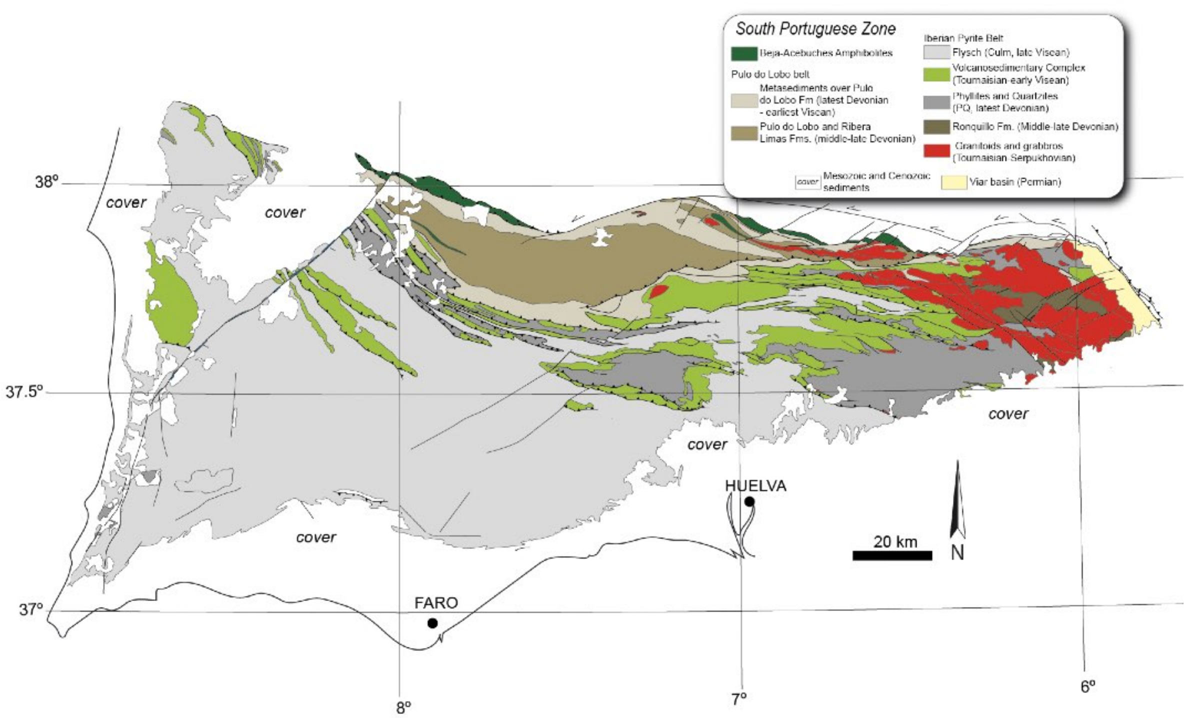

Figure 7. The South Portuguese Zone. The Beja-Acebuches Ambibolites have been interpreted by some authors as evidence of the Rheic suture (after Simancas, 2004)

The SP Zone features marine deposits from the Middle Devonian to the Carboniferous, low-grade metamorphism, general tectonic foliation, and abundant magmatism.

Based on the stratigraphy, most authors distinguish three domains: the Northern Domain or Pulo do Lobo, the Central Domain or Iberian Pyrite Belt and the Southern Domain or Southwest Portuguese. The Northern Domain seems to represent an accretionary prism generated during the subduction of the South Portuguese plate; it was the source area for the Pyrite Belt.

The Pyrite Belt stands out for containing the world's largest accumulation of massive metal sulfide of enormous economic importance (mines of São Domingos, Neves Corvo, Tharsis, Río Tinto or Aznalcollar). Volcanic-hosted massive sulphide mineralization occurs at several stratigraphic horizons within an Early Carboniferous volcano-sedimentary package formed of turbiditic siliciclastic deposits and basaltic, intermediate and silicic volcanic rocks. Volcanic rocks do not show significant temporal or spatial variations and mainly occur as shallow intrusions into wet marine sediments. The sulfide deposits originated during the Lower Carboniferous, in an extensional moment of the basin prior to the Variscan collision; they formed during several hydrothermal episodes of progressively increased temperature that were later reworked by tectonic processes.

The Southwest Portuguese Domain (SWP) represents a paleogeographic position different to that of the Pyrite Belt. Both areas underwent similar evolution during the Devonian but dramatically differed during the Carboniferous. The SWP remained stable during the Carboniferous with no noticeable magmatism. The detrital Devonian sediments were replaced by platform detrital-carbonate sediments until the Upper Namurian when turbiditic materials of the Baixo Alentejo Flysch Group covered them.

The magmatic activity in the SP zones caused two main formations, the Volcanosedimentary Complex of the Pyrite Belt and the composite Sevilla Sierra Norte Batholith.

The Volcanosedimentary Complex consists of volcanic and subvolcanic rocks interlayered with volcanoclastic rocks and detrital and chemical sediments. The volcanism is bimodal, mafic and felsic this with zircon U-Pb ages around 350 Ma.

The Sierra Norte Batholith crops out in the NE of the South Portuguese Zone, intruding the Pulo de Lobo Domain in the west and the Pyrite Belt in the south. It consists of plutonic and subvolcanic rocks of different compositions, from ultramafic cumulates to leucogranites, that can be grouped into four categories: (i) gabbros, diorites and ultramafic rocks, (ii) garnet-bearing monzogranites and subvolcanic granites, (iii) tonalites and granodiorites with microgranular enclaves, (iv) zones of magma mixing and mingling. All but few of these rocks have SHRIMP zircon U-Pb ages around 348 Ma, I.e. which errors of the Volcanosedimentary Complex from the Pyrite Belt.

The field trip

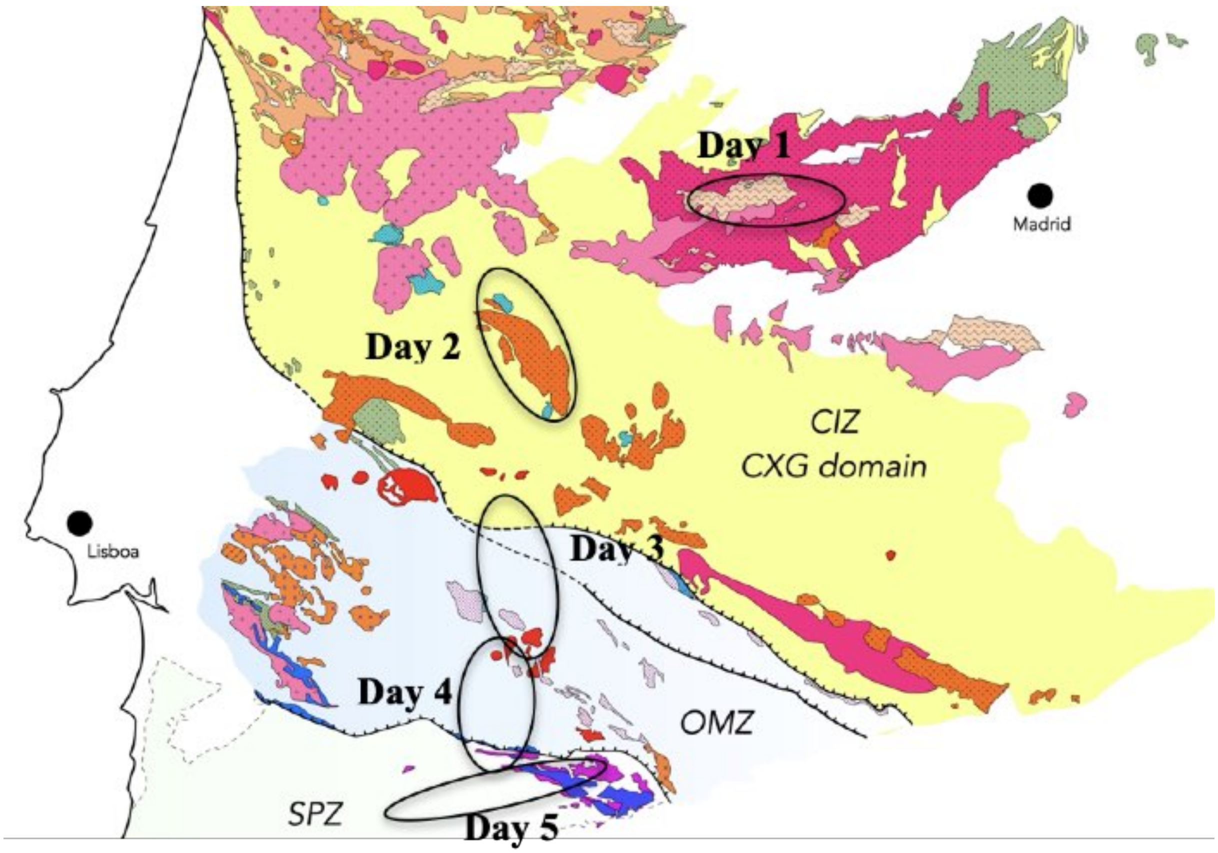

Figure 8.- Areas to be visited

Day One (May 9th): The Avila Batholith

On the first day, we shall visit the Avila Batholith, one of the largest and more complicated of the Iberian Massif.

The batholith is composed of coalesced autochthonous to allochthonous plutons of aluminous biotite ± cordierite bearing granodiorites to monzogranites accompanied by subordinate two-mica ± aluminosilicate ± cordierite granites and leucogranites with ages clustering around 310

Ma. There are several anatectic complexes of various sizes scattered among batholithic granites, the Peña Negra one being the most important. Besides, there are volumetrically insignificant bodies of mafic-ultramafic appinitic rocks always slightly younger than the coeval granites they are spatially related to; their ages cluster around 308 Ma. Several dike swarms of Early Permian (264 Ma) camptonitic lamprophyres cut the peraluminous granites.

<u>Stop 1</u> (40.27623ºN 5.231702ºW). Plataforma de Gredos. About one hour walk into the mountains to the Prado de las Pozas (40.270076ºN 5.246394ºW). The way makes a vertical cross-section of the subhorizontal Hoyos granodiorite unit (Fig. 9), from the bottom, just over the Peña Negra migmatites, to the Prado de la Pozas Mafic Complex, where the interaction between coeval mafic and felsic rocks is displayed (Fig. 10). The Hoyos-type granodiorites are porphyritic rocks composed of K-feldspar megacrysts often with a planar subhorizontal foliation, plus a granodioritic to tonalitic coarse-grained groundmass consisting of andesine-oligoclase, quartz, minor K-feldspar, biotite, often forming sub-centimetric schlierens, and euhedral prisms of cordierite totally or partially pinnitized. They have apatite, monazite, zircon, Fe-Ti oxides and scarce sulfides as accessories.

The mafic rocks are K-rich diorites or gabbro-diorites, which in contrast with most compositionally similar Gredos's rocks, do not show appinitic structures. The mineralogy comprises andesine or labradorite-andesine, hornblende, Mg-rich biotite and locally minor K-feldspar, with titanite, apatite, zircon, and Fe-Ti oxides as accessories.

SHRIMP zircon U-Pb revealed that the two rocks, granodiorites and diorites have 310 ± 3 Ma and 309 ± 2 Ma, respectively.

Figure 9. The Hoyos cordierite-bearing granodiorite. Note the subhorizontal foliation defined by enclaves and K-fsp megacrysts.

Figure 10. Mafic rocks fragmented and invaded by the Hoyos granodiorite

<u>Stops 2</u> (40.404273ºN 5.377684W) and 3 (40.422424ºN 5.310704W). Peña Negra migmatites. We shall see the Peña Negra migmatite series, including the cordierite-bearing metatexites (Fig. 11) and nebulites (Fig. 12) that are the magmatic source for the Hoyos-type adamellites and granodiorites. The road goes down about 900 m in altitude from the Peña Negra Peak to the Piedrahita village, with excellent exposures of the different types of migmatites.

Figure 11. Peña Negra schlieren migmatites. The leucosome consists of qtz + kfsp + oligoclase + cordierite. The melanosome consists of biotite + sillimanite ± ilmenite. Occasionally there are large monomineralic sillimanite or qtz nodules and calc-silicate enclaves

Figure 12. Peña Negra nebulitic migmatites. The bulk composition is similar to the schlieren migmatites, but the melanosome is de-structured and the leucosome consists of cordierite-bearing leucogranites, occasionally segregated in metric to hectometric bodies.

The Peña Negra migmatitic series comprises three varieties: mesocratic, pelitic and leucocratic, the former being, by far, the most abundant and hosting the rest of the rocks found in Peña Negra. Zircon dating (Montero et al., 2004) indicated that anatexis occurred continuously from 352 to 297 Ma, with a maximum at 335 to 305 Ma

Mesocratic migmatites are diatexitic, with a medium to coarse-grained granodioritic to monzogranitic leucosome dominant over a fine-grained restitic melanosome; they contain little or no recognizable mesosome. The leucosome has a hypidiomorphic to granoblastic texture and is mainly composed of quartz, plagioclase (core An_{20-26} rim An_{11-18}), cordierite, subordinate K-feldspar, rare biotite and sillimanite, and occasional garnet and muscovite. The melanosome comprises alternate granoblastic and schistose bands defining a folded foliation; granoblastic layers are formed of quartz + oligoclase ± cordierite ± lozengic sillimanite; schistose layers are formed of biotite and fibrolitic to lozengic sillimanite accompanied by 5 to 10 vol.% of ilmenite and, locally, Fe (Cu) sulfides and graphite. Other accessory minerals are apatite, zircon, monazite, huttonite, and rare xenotime, uraninite and betafite. Accessories, except apatite, mostly appear as inclusions in biotite.

The mesocratic migmatites are divided into three facies: schlieren, nebulitic and transitional, on the basis of their mesoscopic structures. Schlieren migmatites (Fig. 11) still preserve a recognizable compositional leucosome-melanosome banding with visible fold and shear structures. Nebulitic migmatites (Fig. 12) are more homogeneous; the melanosome appears within the leucosome either as small enclaves or diffuse schlierens. Transitional migmatites appear between subauthochtonous granodiorites and nebulitic or, less frequently, schlieren migmatites; they are characterized by the appearance of megacrysts of K-feldspar oriented along the foliation. Despite these differences, the three facies have identical modal and chemical compositions.

Metapelitic migmatites (Fig. 13) consist of fine-grained dark-colored metatexitic migmatites with abundant dyktionitic structures. The mesosome has well-developed granolepidoblastic textures and is composed of dominant quartz and biotite, with subordinate sillimanite, cordierite and plagioclase (An_{17-62}), and rare K-feldspar and muscovite. The leucosome forms thin veins; its major minerals are quartz, K-feldspar, acid oligoclase and rare cordierite, biotite and, locally, muscovite and tourmaline. Accessory minerals are ilmenite, Fe-sulfides, apatite, zircon, monazite and rare huttonite.

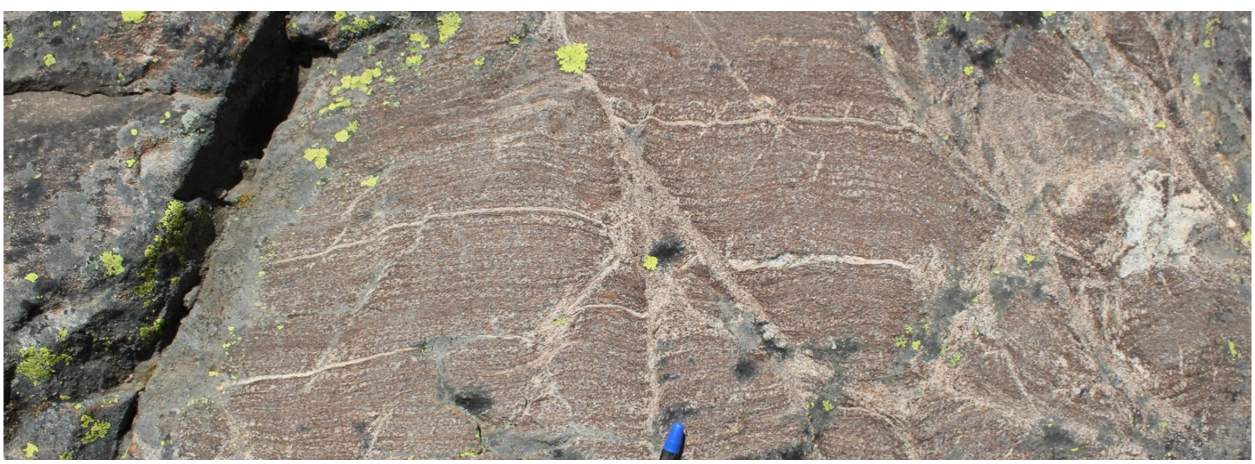

Figure 13.- Metapelitic migmatites with different leucosome generations.

Leucocratic migmatites (Fig. 14) have the same mineralogy as mesocratic migmatites, but the proportion of leucosome is notably higher, and its composition is more leucogranitic. The melanosome appears either as planar streaks or, more commonly, rounded nodules (Ø

~ 10 to 15 cm) generally oriented according to the foliation. For this reason, some authors have called them “nodular granites”.

Figure 14.- Leucocratic migmatites. The nodules comprise biotite ± cordierita ± sillimanite ± muscovite. They are whithin an haplogranitic groundmass

<u>Stop 3</u> (40.460976ºN 5.371652ºW). Almohalla orthogneisses. These are one of the oldest igneous rocks of the Central Iberian Zone (543 ± 3 Ma) and display the three Variscan deformation phases in a single outcrop (Figs. 15 and 16). The orthogneisses are coarse-grained, intensely deformed and recrystallized mesocratic rocks which may locally be slightly migmatised. Textures are gneissose granoblastic, locally oftalmitic. Quartz, plagioclase (An_{23-48}), K-feldspar and biotite are the major minerals; myrmekites are locally abundant. The orthogneisses contain ilmenite, titanite, apatite, zircon and monazite as accessories. The migmatization is usually metatexitic and results in forming 5-10 cm wide veins of fine-grained neosome within the otherwise untransformed orthogneiss. There is no recognizable melanosome. The neosome has almost the same mineralogical and chemical composition as the mesosome; it is composed of large crystals of restitic plagioclase within an aplitic groundmass with abundant micropegmatitic structures.

Figure 15. Subhorizontal fold in the Almohalla orthogneiss (ca. 545 Ma). It is atributted to the Variscan deformation phase II.

Figure 16. Fine-grained neosome developed on a phase III shear zone in the Almohalla orthogneiss.

***Stop 4* (40.390524ºN 5.574678ºW)** (depending on time). Quarry of cordierite-bearing sub-autocthonous granodiorites. These are the most abundant rocks of the Peña Negra Complex after the mesocratic migmatites. They are medium to coarse-grained rocks with a hypidiomorphic granular groundmass composed of quartz, plagioclase (core An_{29-40}, rim An_{12-17}), rare K-feldspar, aluminous biotite, euhedral prisms of cordierite and occasional sillimanite or andalusite, and large megacrysts of K-feldspar. The average modal composition corresponds to a monzogranite or, rarely, a true granodiorite. Accessory minerals are ilmenite, Fe (Cu) sulfides, rare graphite, abundant apatite, zircon and monazite, rare huttonite and occasional xenotime. The granodiorites usually have a planar subhorizontal fabric concordant with the external shape of the body. Shear structures are common, especially at the top and bottom contacts of the plutons, where they grade into transitional migmatites.

Day Two (May 10th)

The second day is devoted to the Cabeza de Araya Batholith (308 to 305 Ma) and the neighbouring Cambrian-Ordovician (ca. 480 Ma) Zarza la Mayor Pluton (Fig. 17).

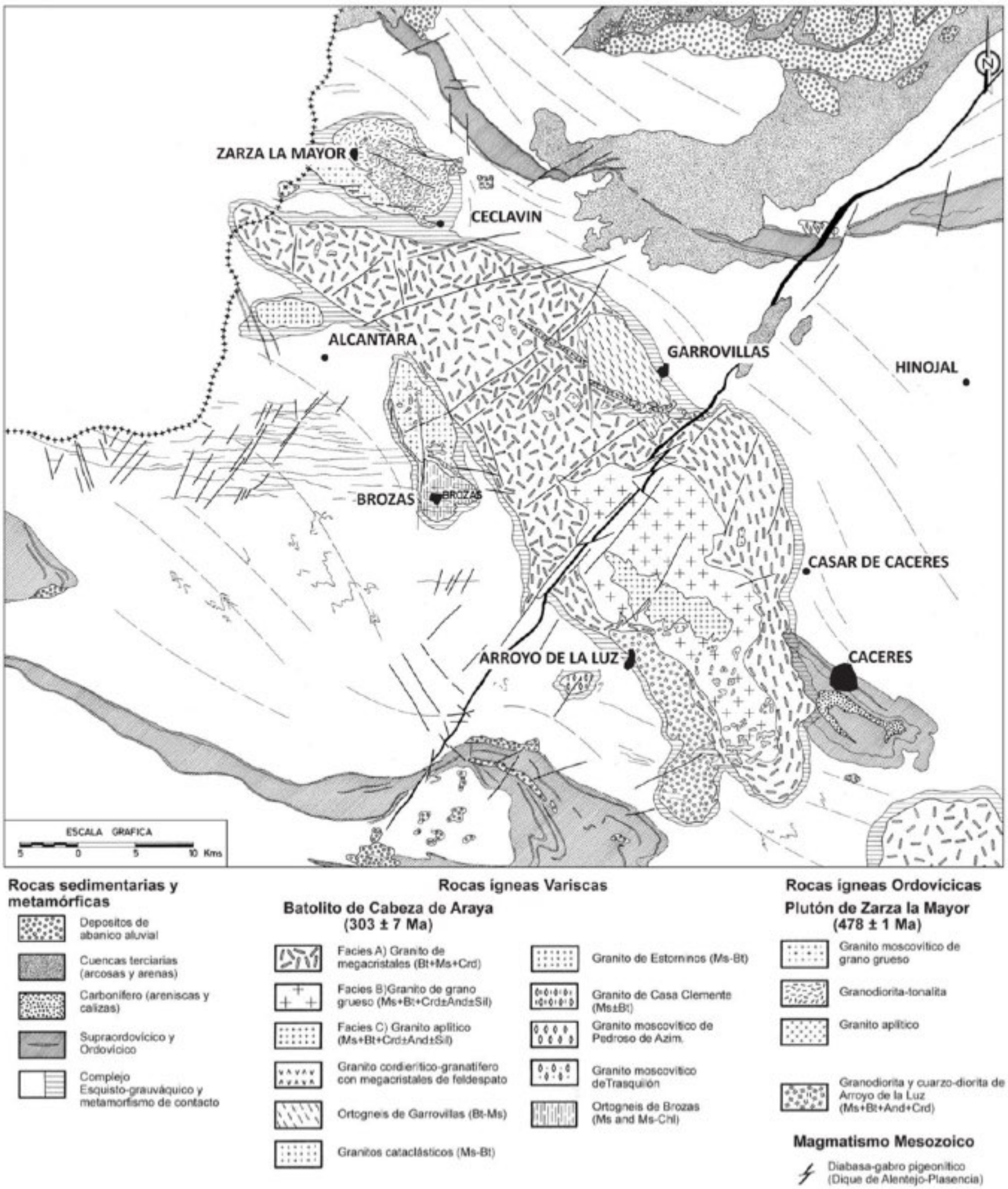

Figure 17. Geological map of the Cabeza de Araya Batholith and its surroundings. After Corretgé (1971)

Cabeza de Araya

Cabeza de Araya is one of the most representative batholiths from the half south of the Central Iberian Zone. It is allochthonous, emplaced within the Schist-Graywacke Complex, developing a contact-metamorphism aureole. The rock types are peraluminous adamellites, granites and leucogranites with abundant cordierite, andalusite or both, arranged to define a marked centripetal zonation (Fig. 17).

The adamellites (customarily called Facies A, Fig. 18) occupy the outer parts of the batholith. They are porphyritic, with abundant K-feldspar megacrysts within a coarse-grained groundmass formed of quartz, perthitic K-feldspar, oligoclase, often with albitic rims, biotite, cordierite, and muscovite as major minerals, plus andalusite, zircon, apatite and scarce Fe-Ti oxides as accessories. The Facias A granites are undeformed except in the middle-east of the batholith, near Garrovillas, where they are affected by fragile shears (Fig. 22).

Towards the centre of the batholith, the adamellites merge gradually into more felsic granites, the so-called Facies B (Fig. 19). These granites are coarse-grained but non-porphyritic, slightly more felsic, and with plagioclase more sodic than the granites from the Facies A. The varietal mineralogy comprises muscovite, biotite and andalusite, locally very abundant. The accessories assemblage includes sillimanite, cordierite, tourmaline, apatite and zircon.

The Facies C (Fig. 20) comprises aplitic muscovite leucogranites with accessory biotite and andalusite. They occupy the central part of the batholith southeast, also appearing in topographic highs dispersed in the batholith. C-type leucogranites are more felsic and less ferromagnesian than the others.

Cross-cutting the batolith there is a 21 km long up to 900 m thick NW-SE dike made up of a garnet-cordierite microgranite with feldspar megacrysts that occasionally show rapakivi textures, Pl (Ab>75) and Qtz, together with garnet and cordierite of restitic origin, plus biotite and locally primary muscovite (Figs. 17 and 21). Provisional monazite dating suggest a 280 ± 5 Ma age.

The granite sequence of Cabeza de Araya is also seen in many other granite bodies in the centre and south of the Central Iberian Zone.

Zarza la Mayor

The Zarza la Mayor pluton bears striking similarities with Cabeza de Araya, despite being more than 170 million years older. As this, Zarza consists of three main facies: biotite tonalite, coarse-grained muscovite ± biotite granite and aplitic leucogranite (Corretgé, 1971). The biotite tonalite constitutes the largest unit of the pluton (Fig. 17). It has a medium-grained hypidiomorphic texture with quartz, plagioclase and biotite as the main minerals and K- feldspar, apatite, Fe-Ti oxides, zircon, titanite, anatase and rutile as accessories. The plagioclase crystals are anhedral to subhedral and locally partially oriented, defining magmatic flow structures. They show a strong zonation with $An_{50–60}$ cores and $An_{6–10}$ rims evidencing intense changes in magma composition during crystallization. The muscovite ± biotite granite is an elongated body, approximately 3 to 4 km wide and 10 km long, located along the southern border of the tonalite. It locally shows a mylonitic foliation that causes gneissic and cataclastic textures. The aplitic leucogranite intrudes the tonalite forming a ring- dyke complex with dykes feeding sills on the cupola of the pluton in a way similar to the Cabeza de Araya Facies C leucogranites. Zarza la Mayor is part of an NW-SE lineament of Cambrian-Ordovician intrusive granitoids that crop out in half south of the Central Iberian Zone (Fig. 6) and seem unaffected, or very little, by the Variscan deformation.

***Stop 1* (39.552501ºN 6.443129ºW)**. Cabeza de Araya, Facies A. It comprises biotite-dominant two-mica adamellites with abundant K-feldspar megacrysts. The adamellites are coarse- to very coarse-grained, with subhedral to euhedral cordierite, generally pinnitized. The megacrysts can be up to 10 cm long, always euhedral. Their concentration varies, reaching such a high proportion that the rock appears holo-feldespathic.

Figure 18. Facies A; note the abundance of K-feldspar megacrysts and cordierite crystals, always pinnitized.

***Stop 2* (39.543451ºN 6.481998ºW)**. Cabeza de Araya. The intermediate Facies B comprises muscovite dominant two-mica granites. They are non-porphyritic and coarse-grained with a hypidiomorphic granular texture. The main mineral phases are K-feldspar, oligoclase-albite, quartz, muscovite and biotite, accompanied by andalusite, which is locally very abundant, and minor cordierite and sillimanite.

Figure 19. Facies B; note the absence of K-feldspar megacrysts. Cordierite is often accompanied by andalusite.

***Stop 3* (39.531241ºN 6.510951ºW)**. Cabeza de Araya, Facies C. It comprises aplitic alaskites and granites with saccharoidal texture and a pale yellow to white colour. The main mineral phases are albite, K-feldspar, quartz, muscovite and subordinate biotite, cordierite, sillimanite, andalusite and tourmaline.

Figure 20.- Facies C. See text for description

Stop 4 ***(39.674007ºN 6.516087ºW)***. Cabeza de Araya. Garnet-cordierite microgranite (Fig. 21)

Figure 21.- Cordierite-garnet granite. The large green spots are cordierite-garnet aggregates. This rock appears as a large NW-SE dike in the middle eastern part of the batholith.

Stop 5 ***(39.709256ºN 6.558740ºW)***. Cabeza de Araya. Garrovilla orthogneisses (Fig. 22).

Figure 22.- In the batholith east appears the Facies A affected by numerous fragile shears, likely related to a late-tectonic event.

***Stop 6* (39.721802ºN 6.891685ºW)**. Alcántara Roman Bridge. Schist Graywacke Complex

Figure 23.- Mesoscopic and exposure aspect of the Schist-Greywacke Complex at the Alcantara Bridge

***Stop 7* (39.721802ºN 6.891685ºW)**. Zarza la Mayor biotite-tonalite (Fig. 24).

Figure 24.- The Zarza la Mayor biotite tonalite. This pluton has the same field relationships as Cabeza de Araya, with differentiated aplites occupying the highs. It is undeformed or with a tenuous subvertical foliation, yet it is c.a. 170 m.y. older tan Araya granites.

Day 3 (May 11th): The boundary between Central Iberia and the Ossa-Morena Zone

The third day will be dedicated to the OMZ-CIZ boundary (stops 1 to 3 in Fig. 25)

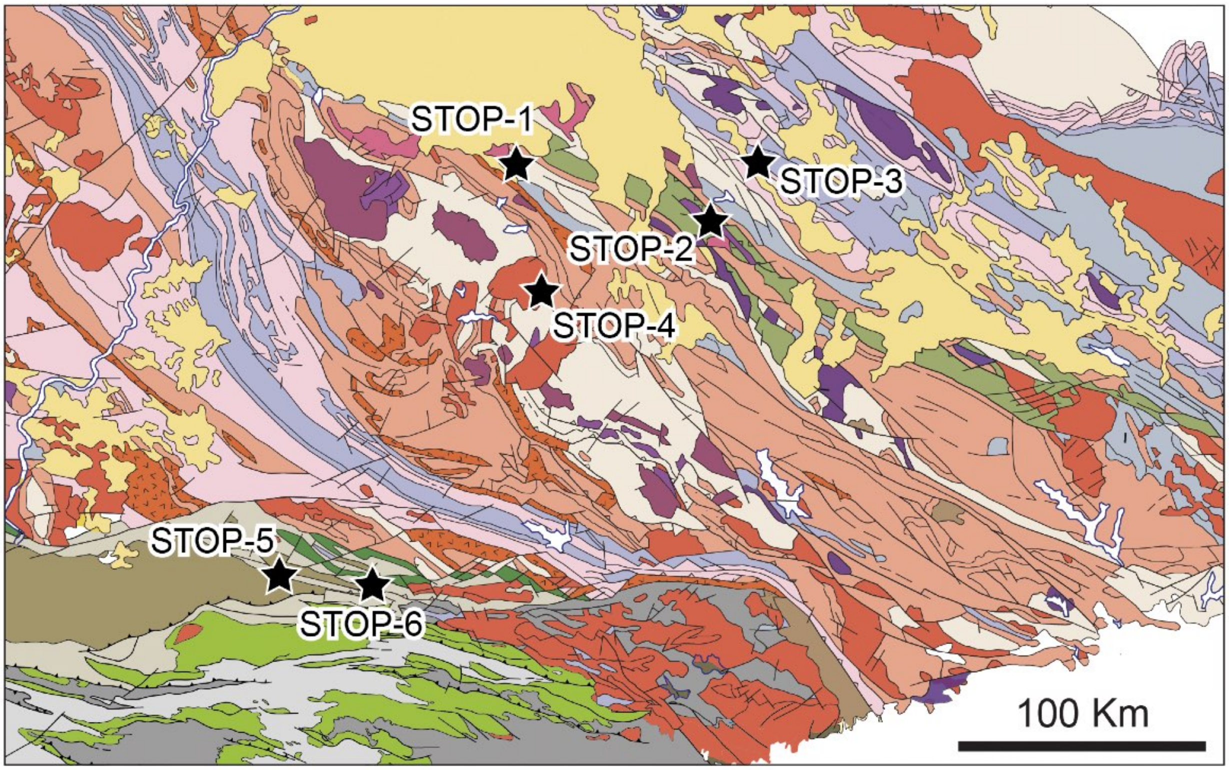

Figure 25. General location of the proposed stops. The geological background corresponds to figures 6 and 7. See Figure 1 and Figure 2 for location within the Iberian Massif and the whole Variscan puzzle.

<u>Stop 1</u> (38.59620ºN, 6.47724ºW): Migmatites, migmatitic gneisses and garnet-bearing amphibolites (retro-eclogites) from the suture unit between the Ossa-Morena and the Central Iberian Zone. The stop starts 3.5 km southeast of Villalba de los Barros along the road EX-361 to Puebla del Maestre, and follows a dirt road directed northwards to a pond (Charca del Pocito Ciego). The exposures consist of different gneisses and amphibolites affected by the Badajoz-Cordoba Shear Zone (BCSZ) (Figs. 26-28). The metamorphic evolution of the BCSZ rocks recorded an early eclogite-facies assemblage (≈1.7 GPa, 700 ºC), evolving later to lower pressure and temperature conditions (exhumation during deformation dominated by ductile, left-lateral simple shearing). The age of the mafic protoliths is Lower Ordovician (c. 483 Ma; Ordóñez-Casado, 1998), while the high-pressure metamorphism has been dated at c. 377 Ma (Abati et al., 2018) and migmatization at c. 340 Ma (Ordóñez-Casado, 1998; Pereira et al., 2012).

There are excellent outcrops of migmatites and migmatitic gneisses at the roadside, showing a NE-dipping mylonitic foliation (cross-section in Fig. 26) with a gently plunging stretching lineation (oriented NW-SE). Shear criteria (SC structures and K-feldspar grains with asymmetric tails) indicate a left-lateral (top-to-the-NW) sense of movement (Fig. 27).

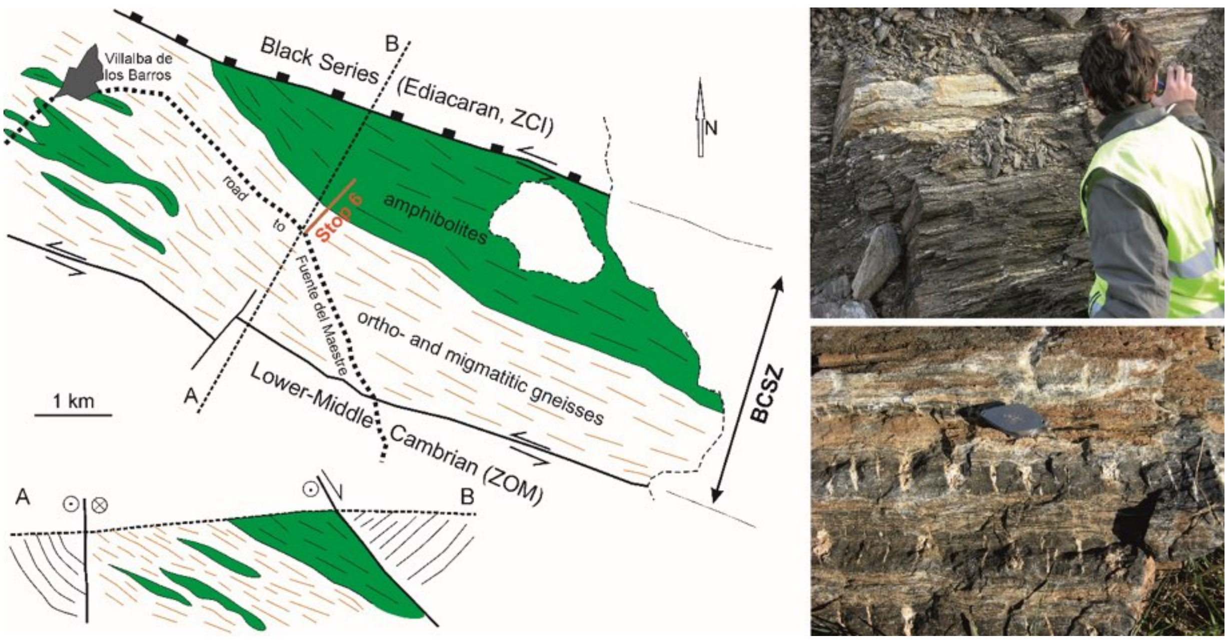

Figure 26. The BCSZ at Villalba de los Barros: schematic map, cross-section and photos of migmatitic gneisses (top-right) and retroeclogitic amphibolites (bottom-right). See Fig. 25 for general location.

Along the first 50 m of the dirt road, large blocks of stretched and boudinaged retro-eclogitic amphibolites are piled up (bottom-right picture in Fig. 26).

A second part of this stop is conceived to observe large blocks of retro-eclogites (garnet-bearing amphibolites; Fig. 28) in a pond, namely, Charca del Pocito Ciego (38° 35’ 58.87” N, 6° 28’ 21.78” W), located 600 m from the roadside following N and NE the dirt road.

Figure 27. Mylonitic orthogneisses with S-C structures and asymmetric tails around K-feldspar porphyroclasts, indicating left-lateral ductile shearing.

Figure 28. Garnet-bearing amphibolite from the Charca del Pocito Ciego.

<u>Stop 2</u> (from 38.504263N, 6.125259W to 38.517889N, 6.143417W; road from Hinojosa del Valle to Hornachos): Top of the BCSZ and contact with the CIZ (south of Los Molinos dam). The topmost exposures of the BCSZ consist here of intermediate-grade metamorphic rocks, mainly orthogneisses and mica-schists. The proposed transect begins at the Ribera del Fresno orthogneiss (c. 475 Ma), a highly deformed body with subhorizontal stretching lineation and pristine S-C structures indicating left-lateral kinematics (Fig. 29, left and Fig. 30). The orthogneisses of the BCSZ vary from peraluminous (Ribera del Fresno) to peralkaline and are related to the pre-Variscan early Ordovician rifting. The seismic reflection profile shows that the NE-dipping foliation suggests that the BCSZ sinks below the CIZ (Fig. 29, right).

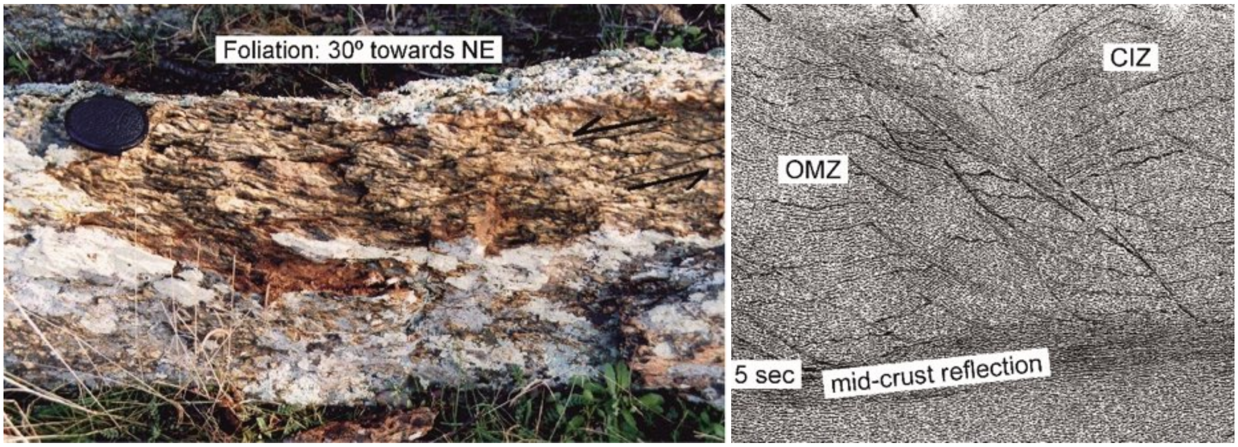

Figure 29. Ribera del Fresno orthogneiss (left), showing S-C structures indicative of left-lateral ductile shearing. Right: Window of the IBERSEIS seismic reflection profile (right) (Simancas et al., 2013) showing how the BCSZ sinks to the NE underneath the CIZ.

Following the road northwards, mica-schists and quartzites crop out, dipping to the NE. In the last 500 m of the cross-section, the schists are affected by semi-brittle structures (pseudo-S-C) that indicate an extensional left-lateral normal fault (Matachel fault, north boundary of the BCSZ), which downthrows the NE block, namely the CIZ. North of the Matachel fault, dark graphite-rich schists and metagreywackes of the late Ediacaran Serie Negra crop out, representing the southernmost CIZ

Figure 30. Outcrop of the Ribera del Fresno orthogneiss in a section parallel to the stretching lineation and perpendicular to the foliation to show the prominent presence of S-C structures indicative of left-lateral ductile shearing

Stop 3** (Hornachos town): Km-scale NE-vergent recumbent synclinal fold, southernmost CIZ (Sierra de Hornachos).* The southernmost CIZ is characterized by km-scale middle-late Devonian recumbent folds (Expósito et al., 2002, Martínez Poyatos et a., 1995), which show opposite vergence to those of the same age in the OMZ. This stop shows one of these large-scale folds (Fig. 31). The observations will be done at three different points, which are described below. The first outcrop to visit corresponds to late Ediacaran Serie Negra rocks (mainly dark schists with some metagreywacke intercalations) exposed at the exit of Hornachos along the road EX-342 (38.555205N, 6.083351W***). The general dip of the main foliation in the Serie Negra here is to the NE, and S0/S1 relationships can be observed, indicating NE-vergence (Fig. 32). On the way back to Hornachos along the road, metarhyolites and metatuffs of the latest Ediacaran-earliest Cambrian Malcocinado formation crop out, showing low dipping foliation (cross-section in Fig. 31) and no clear S0/S1 relationships.

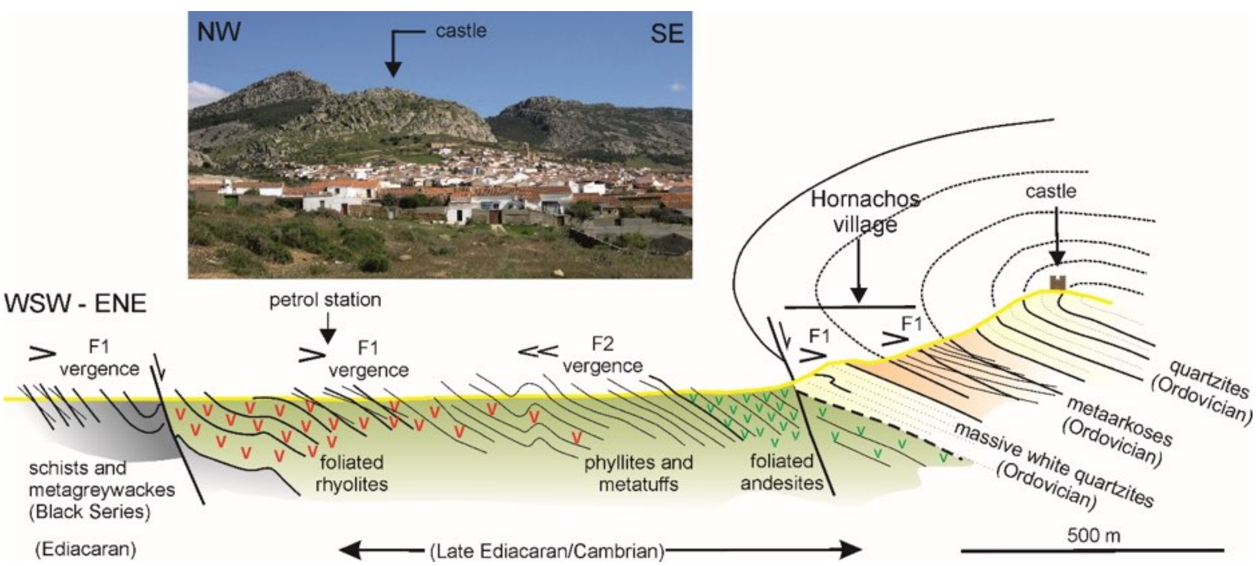

Figure 31. Cross-section of the Hornachos middle-late Devonian recumbent syncline, refolded by late Carboniferous upright folds. The picture over the cross-section shows a view of the hinge of the recumbent fold affecting Lower Ordovician quartzites. See Fig. 25 for location.

Figure 32. Decimetre-scale fold in the Serie Negra indicating NE-vergence for the main deformation. The view is approximately NE-SW and the NE is located to the right.

The second set of observations will be done 1 km north of Hornachos along the road EX-344 (***38.562395N, 6.078179W***), where meta andesites of the Malcocinado formation unconformably overlain by lower Ordovician arkoses and quartzites crop out. The Malco-cinado formation is below a thick white subhorizontal quartzite level (Fig. 33), presumably of Lower Ordovician age. Even though the contact is here locally faulted, it correlates at a regional scale with the Toledanic unconformity that characterizes the CIZ. Some 100 m to the north along the road and above the previous massive white quartzites, meta arkoses crop out, showing pristine S0/S1 relationships (Fig. 34) indicative of NE vergence for the phase 1 folds (cross-section in Fig. 31). Stratigraphically above, new thick quartzite beds draw (panorama) the hinge of the recumbent synclinal fold of the Sierra de Hornachos.

Figure 33. View looking south of a subhorizontal white quartzitic level overlying andesites of the Malcocinado formation and attesting the Toledanic unconformity.

Figure 34. S0/S1 cross-cut relationships in lower Ordovician arkoses showing NE vergence at the normal limb of the recumbent Hornachos syncline.

Finally, on the way back to Hornachos, a short walk to the higher part of the town (***38.558200N, 6.065794W***) will serve to have a panoramic view of the hinge of the km-scale recumbent fold (Fig. 35) with a sub-vertical dip of the S_0.

Figure 35. Panoramic view of the Hornachos recumbent syncline.

Day 4 (May 12th): The boundary between the Ossa-Morena and the South Portuguese Zones

***Stop 4** (38.393478N, 6.536628W): Variscan magmatism, the example of Burguillos del Cerro plutonic complex (Stop 4 in Fig. 25)*

The Burguillos de Cerro plutonic complex crops out over 100 km² in the central part of the Olivenza-Monesterio antiform (Fig. 25 and Fig. 36). It has a rounded outcrop and chiefly comprises ultramafic to mafic layered and gabbroic rocks (Fig. 37).

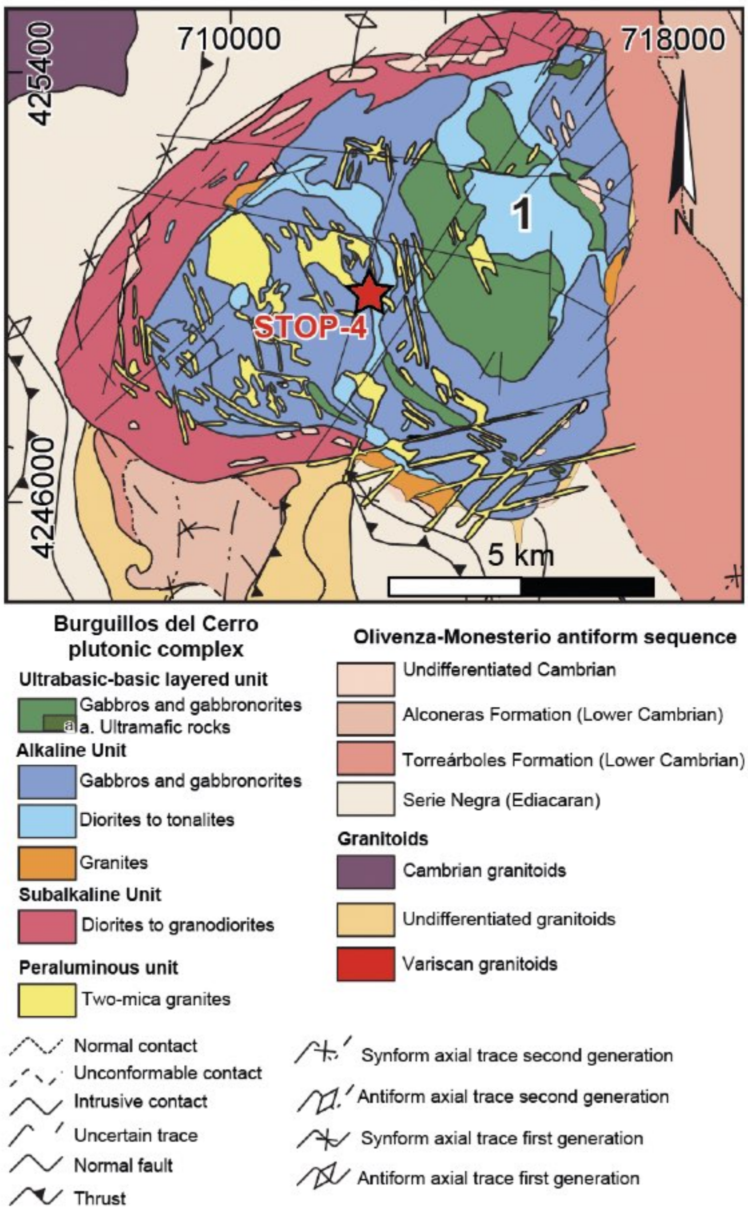

Figure 36. Schematic geological map of the Burguillos del Cerro plutonic complex (from Cambeses, 2015).

Although this plutonic complex is not large, the diversity of rocks and the complexity of the petrogenetic processes it records make it a representative example of the Variscan magmatic event in the Ossa Morena Zone. The Burguillos del Cerro plutonic complex is composed of four main units according to their mineralogical, petrographic, and compositional characteristics: i) Ultrabasic-Basic layered Unit, which comprises cummulitic lherzolites to poikilitic amphibole gabbros and gabbronorites; ii) Alkaline Unit, composed of gabbros and gabbronorites which have a blueish colour, diorites to tonalites and acid syenites and alkali feldspar granites; iii) Subalkaline Unit, comprising diorites to granodiorites and granites and iv) Peraluminous Unit, made up of two-mica peraluminous granites as small bodies and dykes crosscutting the whole complex (Fig. 36).

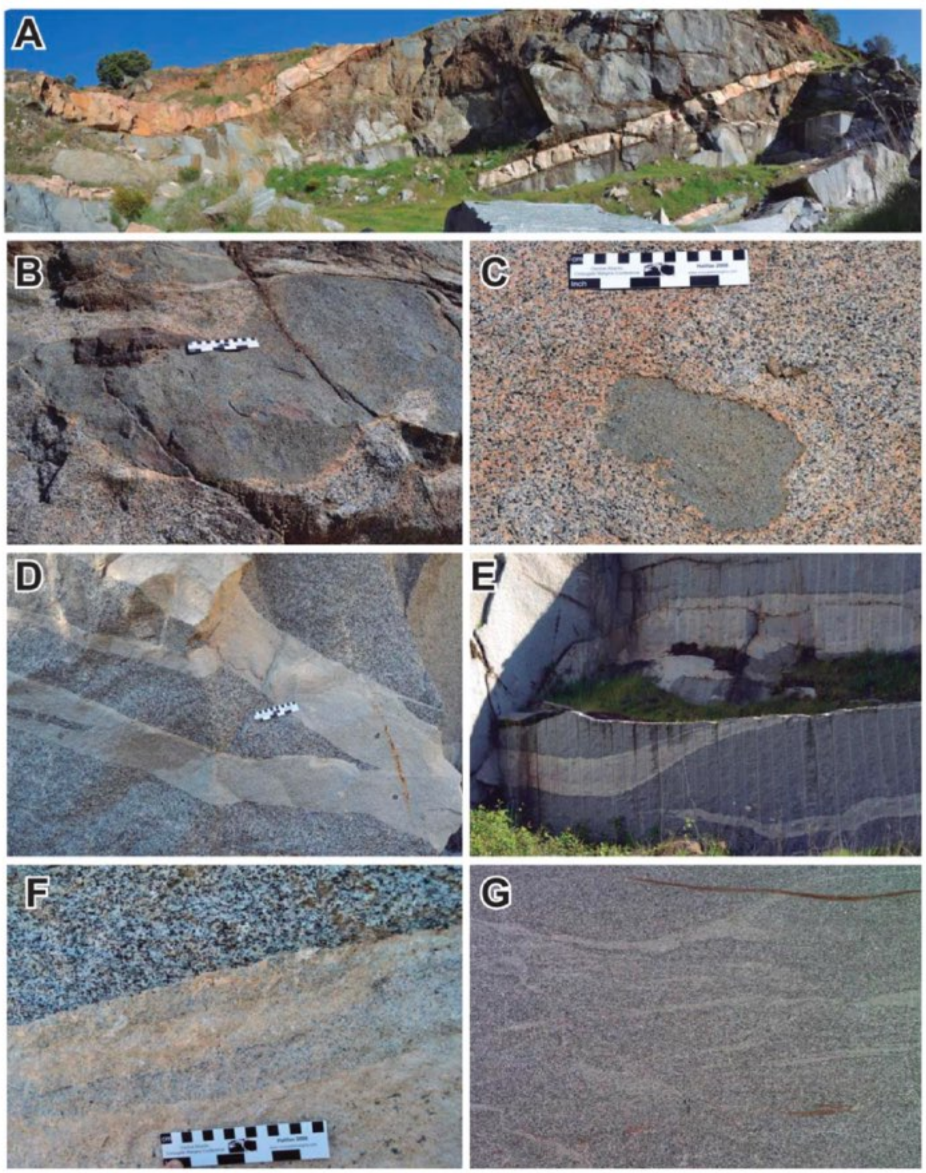

Figure 37. Field relations of the interacion between Peraluminous Unit granite dykes and the Alkaline Unit gabbros and diorites.

The recent U-Th-Pb SHRIMP zircon ages of the four main units range from 338-335 Ma with a mean age of 336 ±1 Ma (Cambeses, 2015). The compositional features of the Burguillos del Cerro magmatism arose from complex petrogenetic processes marked by the mineral chemistry of hydrous ferromagnesian minerals biotite and amphibole, and also plagioclase and whole-rock major and trace elements and Nd-Sr isotopes. One of the most relevant processes is magma hybridization and mingling. The main magma mixing and mingling event involved: (i) alkaline mafic magmas derived from partially melting an enriched lithospheric mantle and (ii) acid peraluminous partial melt derived from the Ossa-Morena Zone basement metasediments. The formers are well represented in the Alkaline Unit, and the laters in The Peraluminous Unit.

In the quarry, we can observe some excellent field relations indicative of the magmatic interaction process between the rocks of the Alkaline and the Peraluminous Units (Fig. 37A). Field relations suggest an intrusion of peraluminous magmas into a mush of mafic to intermediate composition (Fig. 37B and 37C). The branched or curved contact between crustal-derived magmas indicates the melt presence in the mafic component (Fig. 37D and 37E).

Accordingly, the contacts with the more mafic host rock are gradational rather than abrupt (Fig. 37F). The transitional nature of the contact is also evident petrographically in an incremental change in the proportion of the ferromagnesian minerals from the more mafic host to the granitic intrusion (Fig. 37F), which, in places, results in irregular mixed intermediate composition patches (Fig. 37G).

Stops 5 ***(37.941172N, 6.958319W): Internal structure of the Pulo do Lobo Unit at the Aroche-Ciries-El Mustio dirt road (Stop 5 in Fig. 25)***

The dirt road starts close to Aroche and crosses the Pulo do Lobo. Observations at three different locations will show the lithostratigraphy and internal structure of the unit.

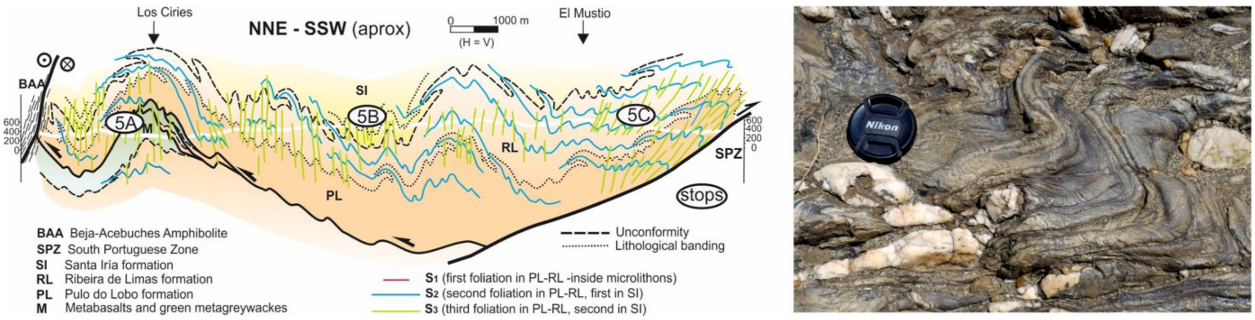

Figure 38. Geological cross-section of the Pulo do Lobo Unit. Right: Superposed Variscan foliations in metasandstones of the Ribeira de Limas formation: S1 foliation preserved inside S2 microlithons, which, in turn, appear deformed by phase 3 folds. See (Pérez-Cáceres et al., 2015) for a discussion of the meaning of this unit.

Stop 5A. Southwards from Aroche, at around 8 km from the start of the dirt road and below the bridge crossing the Ribera del Ciries ***(37.902044N, 7.011379W)***, low-grade metamafic rocks (greenschists) appear intercalated as layers/boudins in the Devonian metasediments of the Pulo do Lobo formation, resembling a tectonic *mélange* (Peramora Melange, interpreted by some authors as an oceanic accretionary prim with remnants of Rheic Ocean floor subduction). However, the zircon U/Pb ages of the metamafic rocks (*ca.* 340 Ma, *i.e.*, Visean) indicate that they are intrusive igneous bodies in the Devonian metasediments, deformed jointly with them during episodes D2 and D3 (see below).

Stop. 5B. Some 7 km SW following the dirt road, slates and greywackes of the so-called Santa Iría formation crop out ***(37.872235N, 7.046961W)***. These rocks rest unconformably over the lower formations of the Pulo do Lobo unit (Pulo do Lobo and Ribeira de Limas formations), being only affected by two penetrative deformations (D2 and D3). The Santa Iría formation crops out in a synform at the central part of the unit (cross-section in Fig. 38). Palynomorphs and detrital zircons suggest Frasnian and/or Famennian ages for the Pulo do Lobo and Ribeira de Limas formations, and late Famennian and/or Tournaisian for the Santa Iría formation.

Stop 5C: Quartz and feldspar metasandstones of the Ribeira de Limas formation (Middle/Upper Devonian) ***(El Mustio forest house, 37.838428N, 7.081291W)***. An S1 foliation is best observed in the metasandstone layers, enclosed in microlithons of a S2 foliation, which, in turn, is folded by a D3 phase. The features of the D1 folds are not known; however, local vergence and stratigraphic polarity relationships indicate that the D2 folds are north-vergent and D3 folds upright to slightly south-vergent.

Stop 6: ***The Beja-Acebuches Amphibolites in Almonaster la Real (Stop 6 in Fig. 25)***

The Beja-Acebuches Amphibolites (BAA) form an E-W belt exposed from Almadén de la Plata (Spain) to Beja (Portugal), and they crop out particularly well in Almonaster la Real. They have MORB geochemistry, ophiolitic pseudo-stratigraphy, an age of *c.* 340 Ma, and a mylonitic deformation.

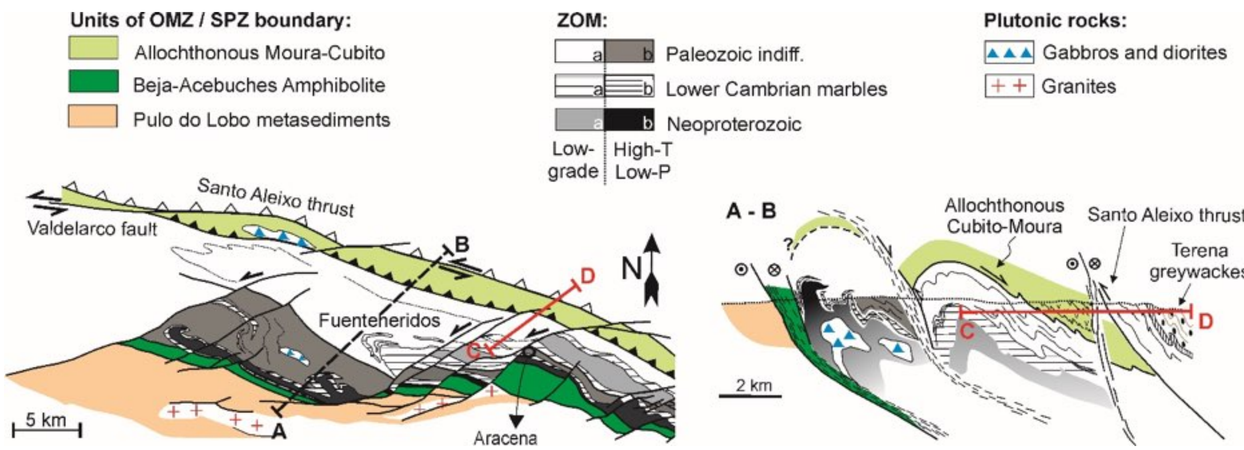

Figure 39. Schematic map and cross-section of the Sierra de Aracena (see location in Fig. 25).

Stop 6A: 3 km east of Almonaster la Real (37.866042N, 6.757612W), on the local road between Santa Ana la Real and Cortegana, migmatites and other high-temperature continental rocks are superposed onto the BAA. On the way to Almonaster la Real, the road offers excellent outcrops of medium-grained amphibolites (Fig. 40, left), with banded grain size variations that can be interpreted, at least in cases of sharp contrast, as a highly deformed alternation of dykes and gabbros. The mylonitic foliation dips to the NNE, and the stretching lineation (though not easily visible) plunges moderately to the east. Asymmetric feldspar tails indicate top-to-the-west shear sense (left-lateral oblique thrusting).

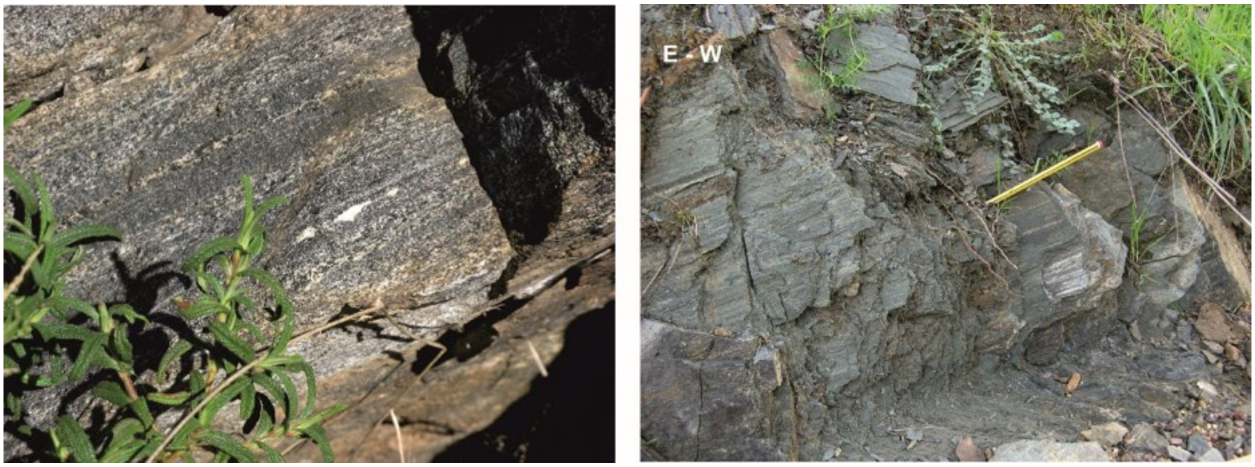

Figure 40. Beja-Acebuches Amphibolites (BAA): banded amphibolites (left) and greenschists with marked stretching lineation (right).

Stop 6B: Almonaster la Real. A small road departs towards La Escalada (37.870273N, 6.782220W). Here, greenschists with prominent stretching lineation are observed (Fig. 40, right), which towards the south, overlie a few meters of mylonitic biotite schists. Finally, a late brittle thrust fault (Fig. 39) superposes the entire BAA unit onto phyllites and quartzites of possible Famennian age (Pulo do Lobo unit). In other sections (*e.g.*, south of Aracena), the foliation locally surrounds less deformed mafic bodies in which igneous textures are preserved. This suggests an inverted polarity for the BAA, with gabbros to the north and overlying volcanic rocks (metabasalts) to the south. Furthermore, in Portugal, west of Serpa, the section of the BAA along the Guadiana river confirms the existence of a large south-vergent anticline with ultramafic rocks in its core (Pérez-Cáceres, et al., 2015).

Day 5 (May 13th): The South Portuguese Zone

As said in the introduction, the SPZ is the southernmost part of the Iberian Massif, which was accreted to the Iberian Autochthonous Terrane during Variscan times (Late Devonian to Late Visean), producing a south-verging, thin-skinned fold-and-thrust belt that propagated southward over a mid-crustal basal detachment (Simancas et al., 2003). In this region, we shall visit the two most important structures: the Iberian Pyritic Belt and the Sierra Norte Batholith.

The Iberian Pyrite Belt

The Iberian Pyrite Belt (IPB) is one of the largest concentrations of volcanogenic massive polymetallic sulphide deposits. It is a 250 km long and 25 to 75 km wide belt composed of volcanic and sedimentary rocks of Late Devonian-Pennsylvanian age. From the footwall to the hanging wall, Schermerhorn (1971) defined three main lithostratigraphic units (Fig. 41):

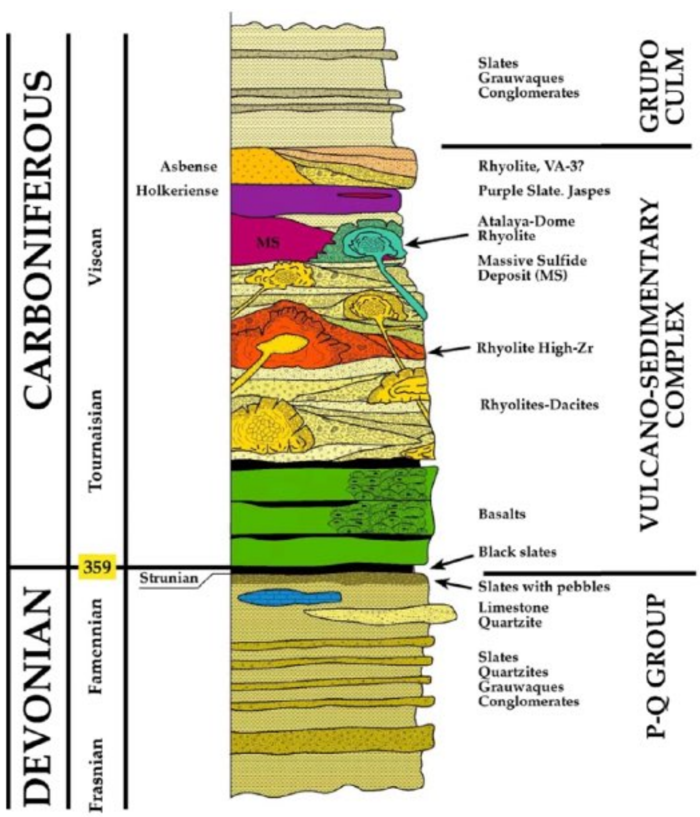

Figure 41. Synthetic stratigraphic column of the Iberian Pyrite Belt in the Rio Tinto anticline (Díez Montes et al., 2017).

- **The Phyllite Quartzite group (PQ)** comprises a >2,000-m-thick detrital sequence dominated by Late Devonian shales and quartzites. It resulted from catastrophic delta fan deposits (Moreno et al., 1996).

- **The Volcano Sedimentary Complex** (CVS) is up to 1,300 m thick of diverse basaltic and rhyolitic lavas and volcaniclastic and sedimentary rocks of Late Famennian to Middle Visean age. It contains the famous polymetallic sulfide and Mn deposits of Aljustrel, Lousal, S. Domingo, Tharsis, Valdelamusa, Rio Tinto and Gerena, some of which are currently exploited. The formation of the volcano-sedimentary complex is attributed to crustal extension, underplating of mafic magmas, and decompression-related melting of the continental crust.
- **The Baixo Alentejo Flysch Group** is a late Visean turbidite-like sequence of slate, greywacke, and conglomerate that diachronically lays on the CVS.

<u>Stop 1</u>: Cerro Colorado open pit of Atalaya-Rio Tinto Mining: Lookout at A-461 route, South La Dehesa de Riotinto village.

Figure 42. Cerro Colorado open pit.

The IPB is the largest mining producer in Spain, and growing player in the European mining sector. In the IPB outcrops more than 85 massive sulfide deposits, an estimate of 1600 Mt of massive sulphide ore and about 2500 t of stock-work ore (Tornos, 2006). The province of Huelva is the main mining region, producing 70% of the region's metallic mining. In this stop, we visit the lookout of Cerro Colorado open pit of the Atalaya Minig Project (Fig. 42) which is one of the three most important mining projects in activity in the SPZ, along with Las Cruces (Gerena) and MATSA Aguas Teñidas (Valdelamusa). In 2021, Atalaya Mining Project produced 56,000 mt of copper in Rio tinto, and processing 15.8 Mt of mineral.

Fig. 43. Location of stops 2 to 6 in El Campillo Area

<u>STOP 2</u>: *Basaltic rocks (spilites) of CVS at El Campillo Park.*

This outcrop is one of the best places to observe spilitized basaltic rocks in the Rio Tinto sector (Fig. 44). The basalts are porphyritic with phenocrysts of plagioclase, clinopyroxene (Ti-augite), and occasional biotite within an aphanitic groundmass. Columnar disjunctions can be distinguished. These volcanic rocks correspond to contemporary sills with the sediments at the base of the CVS. In the Odiel river area, the age of these intrusions is circa 345 Ma (unpublished data).

Figure 44. Basaltic rock (spilites) of the IPB.

STOP 3: ***Phyllites and Quarzites (PQ-Formation) at the South Road crossing A-461- El Campillo village.***

This stop shows shales and quarzites with visible S_1 (see Figure 43).

STOP 4: ***Rhyolites and volcanic breccias North of El Campillo, Road to Aspromin (Fig. 43).***

Outcrop of rhyolites with porphyritic texture and aphanitic matrix. Feldspar phenocrysts. It is interpreted as a dome (Fig.45) broken towards the north, transitioning to volcaniclastic rocks, including fragments of rhyolites, jasper and different types of tuffites. The breccia deposits present a positive grain classification.

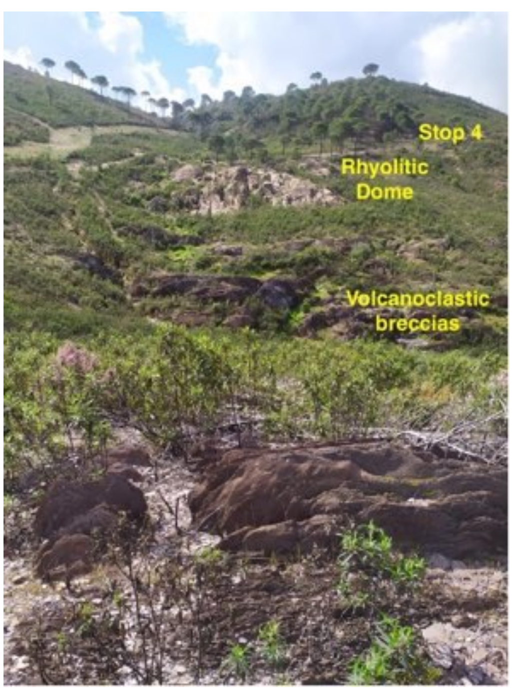

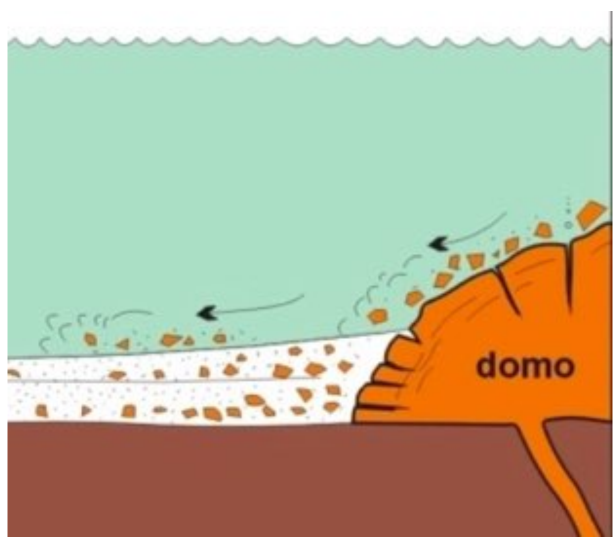

Figure 45. Rhyolitic dome and volcanoclastic breccias in the El Campillo area. Interpretation of dome (Donaire et al., 2008).

***STOP 5**: Purple slates at the north route ASPROMIN- El Campillo*

Purple slate layers serve as a level guide for all the IPB, outcropping at the top of the volcanic sequence (Fig. 46). In purple slates, the color is interpreted by the iron oxidation state of Fe-oxides.

Figure 46. Purple slates.

***STOP 6:** Slates and grawvaques (CULM formation) at the north route ASPROMIN- El Campillo.*

The Culm Group is the uppermost IPB unit and it is interpreted to represent a synorogenic flysch related to the Variscan tectonic event and was partly sourced from the CVS (Moreno, 1993). In this last stop, small outcrop of shales (CULM formation, Fig. 43).

The Sierra Norte Batholith

The Sierra Norte Batholith (SNB, Fig. 47) intrudes into the eastern part of the SPZ (Fig. 7). It is characterized by 10-20 km diameter subvolcanic to epizonal plutonic bodies aligned parallel to the regional structures, intruding a Devonian-Lower Carboniferous pelitic-quartzitic sequence and, occasionally, a Devonian Carboniferous volcaniclastic complex (Simancas 1983). Their compositions include granites, tonalites, and gabbroic rocks, alternating in elongated sheets.

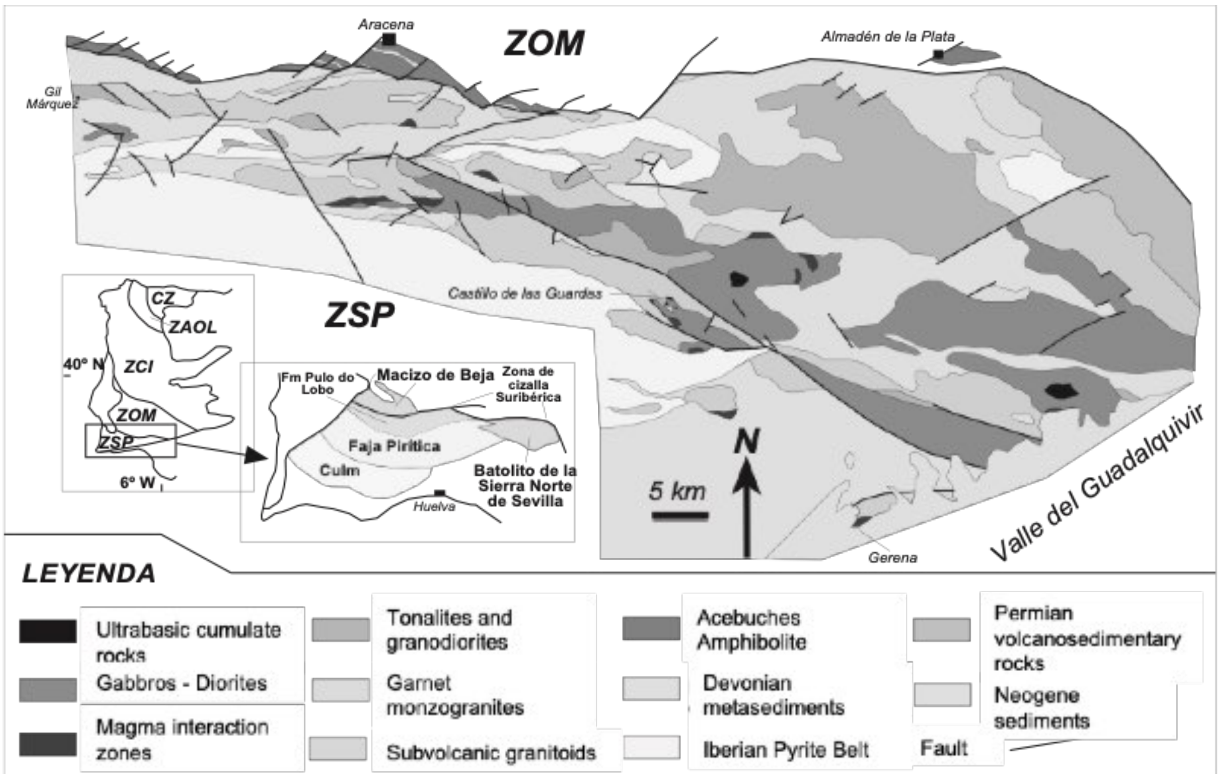

Figure 47. Schematic map of the Sierra Norte Batholith (de la Rosa, 1992).

Acid rocks include granites, tonalites and granodiorites with microgranular enclaves. The textures show a great complexity, from porphyritic, granophyric, orbicular and combinations between them. Among the ferromagnesian minerals, biotite and amphibole (<15%) are the most frequent and are usually retrograded to chlorite + epidote.

These granitoids have ages around 335-340 Ma (de la Rosa et al. 1993). Inherited zircons record ages between 3.0 and 0.6 Ga (de la Rosa et al. 2002); they are, therefore, similar to zircons in the host Serie Negra metasediments, which have ages of 2.1 Ga and older (Shäfer et al. 1993). Nd model ages reported for the granitoids of the Sierra Norte Batholith are in the range of 1.1 to 1.3 Ga (de la Rosa and Castro, 2004). The calc-alkaline suite has a typical signature of subduction-related magmatism, as seen in the American Andes and Sierra Nevada batholiths. We shall visit two prominent locations: Castillo de las Guardas and Gerena.

STOP 7 ***(optional): Ultramafic cumulates and hb-diorites of the Sierra Norte Batholith*** *at the* ***Castillo de las Guardas- El Pedrosillo road***

In the Castillo de las Guardas Sector, cumulate rocks (peridotites and horblendites) (Fig. 48) and anorthosite layered gabbros outcrop in bodies 20-500 m in size and with clear contacts with the host hornblende diorites. Abundant masses of differentiated dioritic pegmatoids of 10-20 cm in size are frequently near contact with cumulate rocks.

Figure 48. Lherzolitic cumulate rocks in the Castillo de las Guardas area

STOP 8*:* ***Magma Interaction Zone. Gerena Massif at the Palace Quarry. Gerena village.***

The Gerena Massif is near Seville in the Guadalquivir Basin (Castro et al. 1990). Complex relationships of felsic and mafic magmas characterize this massif. Pillow-like bodies and syn-plutonic dykes of mafic magma intruded into felsic magma chambers resulting in hybrid tonalite-granodiorite rocks. The 'interaction zone' is in the southern part of the massif, cropping out in several east-west orientated quarries near the village of Gerena (Fig. 49). Several types of rock can be distinguished in the Gerena Interaction Zone (Figs. 50).

1. Pillow-like bodies
2. Ocellic tonalitic enclaves
3. Syn-plutonic tonalitic dykes
4. Hybrid granodiorites
5. Synplutonic quarz diorite-tonalite enclaves

Figure 49. Quarries of magma interaction zone in the Gerena village.

Figure 50. Magma interaction

a) Pillow-like masses
b) Ocellic enclaves
c) Syn-plutonic dykes
d) Syn-plutonic enclave with chilled margin

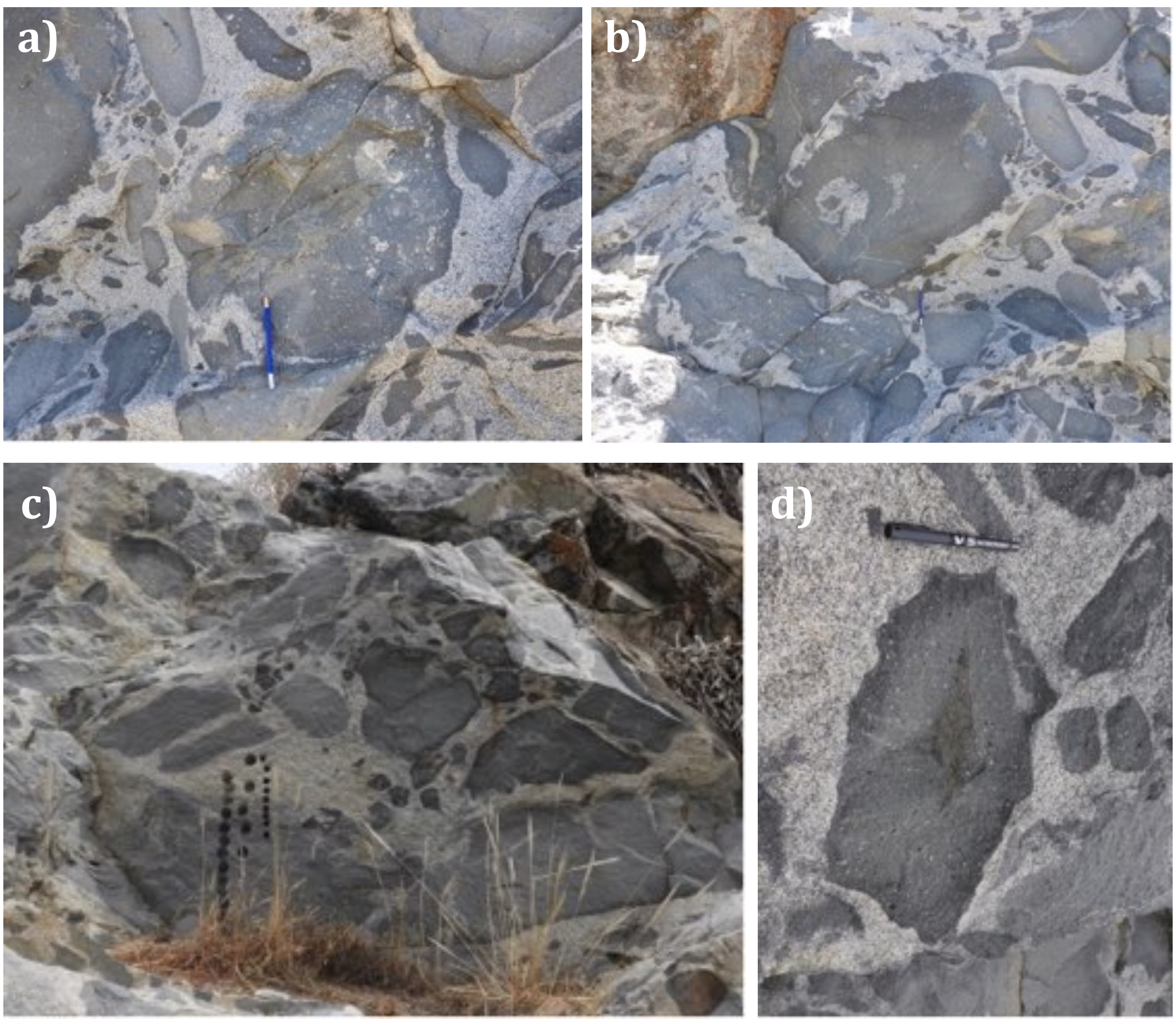

Field relationships indicate that mafic magma was injected into a felsic magma chamber. Intrusion took place mainly as syn-plutonic dykes and liquid, pillow-like globules (Fig.50a), and most of the dykes were disrupted by the magmatic flow. Extensive mingling-mixing zones existed between these magmas, as evidenced by mineral textures and compositions that indicate episodic crystallization histories and hybridization.

The mixing process occurred episodically in response to the intermittent input of mafic magma into the felsic chamber. This idea is supported by the appearance, in the same place, of evolved hybrid facies resulting from complete mixing with non-mixed syn-plutonic bodies with sharp contacts and chilled margins. The process is schematically shown in Fig. 51.

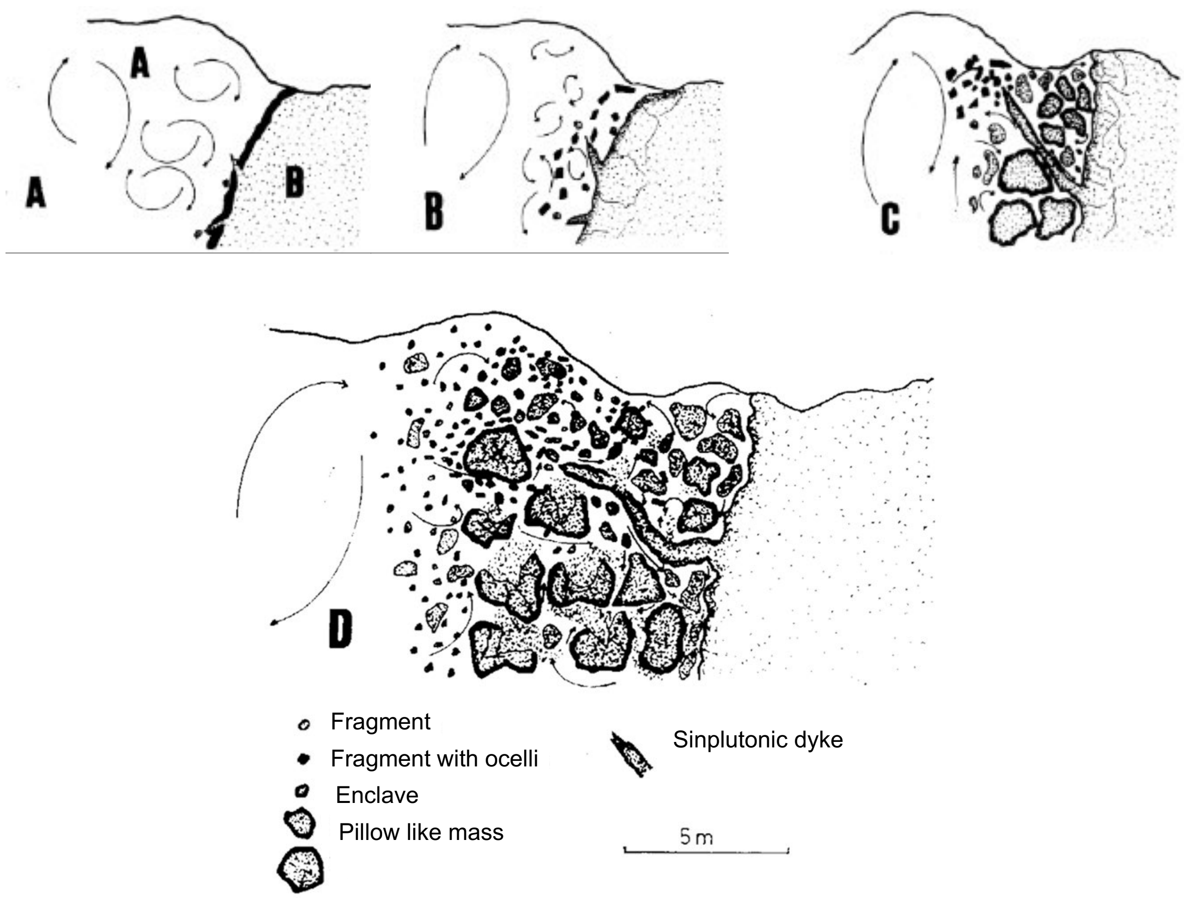

Figure 51. Schematic evolution of the magma mixing phenomena in the Gerena Interaction Zone.

Selected references:

References mentioned in the text and recommended readings

Abati, J., Arenas, R., Díez Fernández, R., Albert, R., Gerdes, A. (2018). Combined zircon U-Pb and Lu-Hf isotopes study of magmatism and high-P metamorphism of the basal allochthonous units in the SW Iberian Massif (Ossa-Morena complex). Lithos 322, 20–37

Arenas, R., Diez Fernandez, R., Rubio Pascual, F., J., Sanchez Martinez, S., Martin Parra, L.M., Matas, Jeronimo, Gonzalez del Tanago, J., Jimenez-Diaz, A.A., Fuenlabrada, J.M., Andonaegui, P., and Garcia-Casco, A. (2016). The Galicia-Ossa-Morena Zone: Proposal for a new zone of the Iberian Massif. Variscan implications. Tectonophysics 681, 135–143.

Ayarza, P. et al. (2021). Evolution of the Iberian Massif as deduced from its crustal thickness and geometry of a mid-crustal (Conrad) discontinuity. Solid Earth 12, 1515-1547. 10.5194/se-12-1515-2021

Azor, A., Rubatto, D., Simancas, J.F., González Lodeiro, F., Martínez Poyatos, D., Martín Parra, L.M., Matas, J., (2008). Rheic Ocean ophiolitic remnants in southern Iberian questioned by SHRIMP U-Pb zircon ages on the Beja-Acebuches amphibolites. Tectonics 27, TC5006, 10.1029/2008TC002306

Bea, F., Montero, P. & Zinger, T. (2003). The Nature and Origin of the Granite Source Layer of Central Iberia: Evidence from Trace Element, Sr and Nd Isotopes, and Zircon Age Patterns. Journal of Geology 111, 579-595.

Bea, F., Montero, P., Talavera, C. & Zinger, T. (2006). A revised Ordovician age for the oldest magmatism of Central Iberia: U-Pb ion microprobe and LA-ICPMS dating of the Miranda do Douro orthogneiss. Geologica Acta 4, 395-401.

Bea, F., Montero, P., González-Lodeiro, F., and Talavera, C. (2007). Zircon Inheritance Reveals Exceptionally Fast Crustal Magma Generation Processes in Central Iberia during the Cambro-Ordovician. Journal of Petrology 48, 2327–2339.

Bea, F., Gallastegui, G., Montero, P., Molina-Palma, J.F., Scarrow, J.H., Cuesta, A., and Gonzalez-Menendez, L. (2021). Contrasting high-Mg, high-K rocks in Central Iberia: the appinite - vaugnerite conundrum and their (non-existent) relation with arc magmatism. Journal of Iberian Geology https://doi.org/10.1007/s41513-020-00152-x.

Boogaard, M van den (1963) Conodonts of Upper Devonian and Lower Carboniferous age from Southern Portugal. Geol en Minjbown, año 42: 248-259.

Booth-Rea, G. et al. (2006). HP–LT Variscan metamorphism in the Cubito-Moura schists (Ossa-Morena Zone, southern Iberia). Comptes Rendus Geoscience 338, 1260-1267 10.1016/j.crte.2006.08.001

Cambeses, A., Scarrow, J. H., Montero, P., Molina, J. F., & Moreno, J. A. (2015). SHRIMP U–Pb zircon dating of the Valencia del Ventoso plutonic complex, Ossa-Morena Zone, SW Iberia: Early Carboniferous intra-orogenic extension-related 'calc-alkaline'magmatism. Gondwana Research, 28(2), 735-756.

Cambeses, A., Scarrow, J. H., Montero, P., Lázaro, C., & Bea, F. (2017). Palaeogeography and crustal evolution of the Ossa–Morena Zone, southwest Iberia, and the North Gondwana margin during the Cambro-Ordovician: a review of isotopic evidence. International Geology Review, 59(1), 94-130.

Cambeses, A., Montero, P., Molina, J. F., Hyppolito, T., & Bea, F. (2019). Constraints of mantle and crustal sources and interaction during orogenesis: a zircon SHRIMP U-Th-Pb and O isotope study of the 'calc-alkaline'Brovales pluton, Ossa-Morena Zone, Iberian Variscan Belt. Lithos, 324, 661-683.

Cambeses, A., Molina, J. F., Morales, I., Lázaro, C., Moreno, J. A., Montero, P., & Bea, F. (2021). Compositional evolution of the Variscan intra-orogenic extensional magmatism in the Valencia del Ventoso Plutonic Complex, Ossa-Morena Zone (SW Iberia): a view from amphibole compositional relationships. Minerals, 11(4), 431.

Castro A, de la Rosa JD, Stephens WE (1990) Magma mixing in the subvolcanic environment: petrology of the Gerena interaction zone near Seville, Spain. Contribution Mineral Petrol 105:9-26. https://link.springer.com/article/10.1007/BF00306405

Castro, A., Fernández, C., De la Rosa, J., Moreno-Ventas, I., Rogers, G., (1996). Significance of MORB-derived Amphibolites from the Aracena Metamorphic Belt, Southwest Spain. J.Petrol. 37, 235-260, 10.1093/petrology/37.2.235

Chichorro, M. et al. (2008). Cambrian ensialic rift-related magmatism in the Ossa-Morena Zone (Évora–Aracena metamorphic belt, SW Iberian Massif): Sm–Nd isotopes and SHRIMP zircon U–Th–Pb geochronology. Tectonophysics 461, 91-113. 10.1016/j.tecto

Corretgé, L. G. (1971). Estudio petrológico del batolito de Cabeza de Araya (Cáceres). Tesis. Univ. Salamanca 453p.

Crespo-Blanc A, Orozco M (1988) The Southern Iberian Shear Zone: A major boundary in the Hercynian folded belt. Tectonophysics 148: 221-227. https://www.sciencedirect.com/science/article/pii/0040195188901308

de La Rosa, J.D. (1992) Petrología de las rocas básicas y granitoides del Batolito de la Sierra Norte de Sevilla. Zona Surportuguesa. Macizo Ibérico. Unpublished Doctoral Thesis, Univ. of Sevilla, 312 pp.

de la Rosa JD, Rogers G, Castro A (1993) Relaciones 87Sr/86Sr de Rocas Básicas y Granitoides del batolito de la Sierra Norte de Sevilla. Rev Soc Geol España 6: 141-149.

de la Rosa, J.D., Jenner, G. A. & Castro, A. (2002). A study of inherited zircons in granitoid rocks from the South Portuguese and Ossa-Morena Zones, Iberian Massif: support for the exotic origin of the South Portuguese Zone. Tectonophysics 352, 245-256.

de la Rosa JD, Castro A (2004). Magmatismo de la Zona Sudportuguesa. In: Geología de España. (Vera, J.A. Ed. Pral.). Sociedad Geológica de España; Instituto Geológico y Minero de España pp:215-222. ISBN: 84-7840-546-1.

Díez Montes A, Bellido F, Sánchez-García T, García J (2017). Lithogeochemistry of volcanic rocks in the Rio Tinto Mne, Iberian Pyrite Belt (Huelva, Spain). Informes Técnicos Nº9 IGME. 51 pp. https://www.igme.es/Publicaciones/publiFree/ProMine/Informe%20técnico%20número%209.pdf

Donaire Romero, T., Valenzuela Aznar, A., Pascual Martínez, E. (2008). Evidencias de vulcanismo antiguo en la cuenca minera: el puente de los Cinco Ojos (norte de Zalamea la Real). In: Olías Álvarez, M., et al.: "Geología de Huelva : lugares de interés geológico". 2ª ed. Huelva : Universidad de Huelva: 104-105

Expósito, I., Simancas, J.F., González Lodeiro, F., Azor, A., Martínez Poyatos, D., (2002). Estructura de la mitad septentrional de la Zona de Ossa-Morena: deformación en el bloque inferior de un cabalgamiento cortical de evolución compleja. Rev. Soc. Geol. España 15, 3-14, https://sociedadgeologica.org/publicaciones/revista-sge/

Fernández, C., Díaz Azpiroz, M., Castro, A., López, S., Fernández Caliani, J.C., Moreno-Ventas, I., (2004). El contacto entre las zonas de Ossa Morena y Sudportuguesa. Características y significado de la banda metamórfica de Aracena, en su sector central entre Aroche y Aracena (Huelva). J. Iberian Geol. 30, 23-51, https://revistas.ucm.es/index.php/JIGE/issue/view/JIGE040412

Gibbons, W., and Moreno, T. (eds.), 2002. The Geology of Spain. The Geological Society of London, 613 p.

Gómez Pugnaire, M.T., Azor, A., Fernández-Soler, J.M., López Sánchez-Vizcaíno, V., (2003). The amphibolites from the Ossa-Morena/Central Iberian Variscan Suture (Southwestern Iberian Massif): geochemistry and tectonic interpretation. Lithos 68, 23-42, 10.1016/S0024-4937(03)00018-5

IGME, (2004). Mapa Geológico de España 1:2.000.000, https://www.igme.es

Julivert M. (1971). L'evolution structurale de l'arc asturien. In Histoire structurale du Golfe de Gascogne, t. 1 Publ. Inst. Français Pétrole. E. Technip.

Julivert M, Fontboté JM, Ribeiro A, Conde LE. (1972) Mapa Tectónico de la Península Ibérica y Baleares, escala 1:1.000.000. IGME, memoria explicative

Julivert, M., Fontboté, J., Ribeiro, A. and Conde, L. (1974). Memória explicativa del Mapa Tectonico de la Peninsula Iberica y Baleares: Inst. Geol. Min., España.

Leistel JM, Marcoux E, Thiéblemont D, Quesada C, Sánchez A, Almodóvar GR, Pascual E, Sáez R. (1998). The volcanic-hosted massive sulphide deposits of the Iberian Pyrite Belt. Mineralium Deposita 33:2-30. https://link.springer.com/article/10.1007/s001260050130

López Sánchez-Vizcaíno, V., Gómez-Pugnaire, M.T., Azor, A., Fernández-Soler, J.M., (2003). Phase diagram sections applied to amphibolites: A case study from the Ossa-Morena/Central Iberian Variscan Suture (Southwestern Iberian Massif). Lithos 68, 1-21, 10.1016/S0024-4937(03)00017-3

López-Guijarro, R. et al. (2008). Ediacaran–Palaeozoic tectonic evolution of the Ossa Morena and Central Iberian zones (SW Iberia) as revealed by Sm–Nd isotope systematics. Tectonophysics 461, 202-214. 10.1016/j.tecto.2008.06.006

Lotze, F., (1945). Zur gliederung der Varisziden der Iberischen Meseta: Geotekt. Forsch., 6, p. 78-92.

Martinez Catalán, J.R., Aller, J., Alonso, J.L., and Bastida, F. (2008). The Iberian Variscan orogen. pp. 13–30.

Martínez Poyatos, D., Simancas, J.F., Azor, A., González Lodeiro, F. (1995). La estructura del borde meridional de la Zona Centroibérica en el sector suroriental de la Provincia de Badajoz. Rev. Soc. Geol. España 8, 41-50, https://sociedadgeologica.org/publicaciones/revista-sge/

Matte, P. (2001). The Variscan collage and orogeny (480-290 Ma) and the tectonic definition of the Armorica microplate: a review. Terra Nova 13, 122–128.

Mitjavila, J., Marti, J. & Soriano, C. (1997). Magmatic Evolution and Tectonic Setting of the Iberian Pyrite Belt Volcanism. J. Petrology 38, 727-755.

Montero, P., Talavera, C., Bea, F., González-Lodeiro, F., and Whitehouse, M.J. (2009). Zircon geochronology and the age of the Cambro-Ordovician rifting in Iberia. Journal of Geology 117, 174–191.

Montero, P., Bea, F., Zinger, T.F., Scarrow, J.H., Molina, J.F., and Whitehouse, M.J. (2004). 55 Million Years of Continuous Anatexis in Central Iberia: Single Zircon Dating of the Peña Negra Complex. Journal of the Geological Society 161, 255–264.

Moreno, C., S. Sierra, and Saez R. (1996). Evidence catastrophism at the Famennian-Dinantian boundary in the Iberian Pyrite Belt. In Recent Advances in Lower Carboniferous Geology, edited by P. Strongen, I. D. Sommerville, and G. L. Jones, Geol. Soc. Spec. Publ., 107, 153–162. https://www.lyellcollection.org/doi/10.1144/GSL.SP.1996.107.01.12

Mitjavila J, J. Marti J and C. Soriano C. (1997). Magmatic evolution and tectonic setting of the Iberian Pyrite Belt volcanism. J. Petrology vol 727 – 755. https://academic.oup.com/petrology/article/38/6/727/1560481

Munha J. (1990). Metamorphic evolution of the South Portuguese/Pulo do Lobo Zone. In Dallmeyer RD & Martínez García E (eds) Pre-Mesozoic Geology of Iberia. Springer -Verlag. Berlin Heidelberg: 363-367. https://link.springer.com/chapter/10.1007/978-3-642-83980-1_25

Murphy, J.B., Keppie, J.D., Nance, R.D., and Dostal, J. (2010). Comparative evolution of the Iapetus and Rheic Oceans: A North America perspective. Gond. Research 17, 482–499.

Oliveira J.T. (1990). Stratigraphy and Synsedimentary Tectonism. In Dallmeyer RD & Martínez García E (eds.) Pre-Mesozoic Geology of Iberia. Springer -Verlag. Berlin Heidelberg: 334-347. https://link.springer.com/chapter/10.1007/978-3-642-83980-1_23

Ordoñez Casado, B. (1998). Geochronological studies of the Pre-Mesozoic basament of the Iberian Massif: the Ossa-Morena Zone and the Allochthonous Complexes within the Central Iberian Zone. Ph. D. Thesis, ETH Zurich: 235 p

Pereira, M.F., Linnemann, U., Hofmann, M., Chichorro, M., Solá, A.R., Medina, J., Silva, J.B. (2012). The provenance of Late Ediacaran and Early Ordovician siliciclastic rocks in the Southwest Central Iberian Zone: constraints from detrital zircon data on northern Gondwana margin evolution during late Neoproterozoic. Precambrian Res. 192–195, 166–189.

Perez-Estaún, A., Bastida, F., Martínez Catalán, J.R., Gutierrez Marco, J.C., Marcos, A. & Pulgar, J.A. (1990). West-Asturian-Leonese Zone: Stratigraphy. In: Pre-Mesozoic Geology of Iberia (R.D. Dallmeyer & E. Martínez-García, Eds.). Springer-Verlag, Berlin 92-102.

Pérez-Estaún, A. and Bea, F., (chapter eds.) (2004). Macizo Ibérico. in: Vera, J.A., (volume ed.), Geología de España. SGE-IGME, Madrid, pp. 19–230.

Pérez-Cáceres, I., Martínez Poyatos, D., Simancas, J.F., Azor, A. (2015). The elusive nature of the Rheic Ocean suture in SW Iberia. Tectonics 34, 2429-2450, 10.1002/2015TC003947

Ponce, C., Simancas, J.F., Azor, A., Martínez Poyatos, D., Booth-Rea, G., Expósito, I. (2012). Metamorphism and kinematics of the early deformation in the Variscan suture of SW Iberia. J. Met. Geol. 30, 625-638, 10.1111/j.1525-1314.2012.00988.x

Quesada C. (1991). Geological constraints on the Paleozoic tectonic evolution of tectonostratigraphic terranes in the Iberian Massif. Tectonophysics 185: 225-245. https://www.sciencedirect.com/science/article/pii/004019519190446Y

Quesada, C. (1998). A reappraisal of the structure of the Spanish segment of the Iberian Pyrite Belt. Mineral. Deposita 33, 31–44. https://link.springer.com/article/10.1007/s001260050131

Quesada, C., and Oliveira, J.T., (eds.) (2019), The Geology of Iberia: A Geodynamic Approach. Springer Nature, Switzerland, Volumes I and II

Rubio-Ordóñez, A., Valverde-Vaquero, P., Corretgé, L.G., Cuesta-Fernández, A., Gallastegui, G., Fernández-González, M., and Gerdes, A. (2012). An Early Ordovician tonalitic–granodioritic belt along the Schistose-Greywacke Domain of the Central Iberian Zone (Iberian Massif, Variscan Belt). Geological Magazine 149, 927–939.

Sanchez-Garcia, T., Bellido, F. & Quesada, C. (2003). Geodynamic setting and geochemical signatures of Cambrian-Ordovician rift-related igneous rocks (Ossa-Morena Zone, SW Iberia). Tectonophysics 365, 233-255.

Schäfer, HJ., Gebauer, D., Nägler, T.F. et al. (1993). Conventional and ion-microprobe U-Pb dating of detrital zircons of the Tentudía Group (Serie Negra, SW Spain): implications for zircon systematics, stratigraphy, tectonics and the Precambrian/Cambrian boundary. Contr. Mineral. and Petrol. 113, 289–299. https://link.springer.com/article/10.1007/BF00286922

Schermerhorn L.J.G. (1971). An outline stratigraphy of the Iberian Pyrite Belt. Bol Geol Min 82: 239-268.

Simancas J.F. (1983). Geología de la extremidad oriental de la Zona Sudportuguesa. Tesis Doctoral. Univ Granada, 439 pp.

Simancas, J.F. (2004). La Zona Sudportuguesa: Estructura. In: Vera, J.A. (ed.). Geología de España, SGE-IGME, Madrid, Spain, 211-215

Simancas, J.F., (2019). Variscan Cicle. in: Quesada, C., and Oliveira, J.T., (eds.), The Geology of Iberia: A Geodynamic Approach. Springer Nature, Switzerland, pp. 1–26

Simancas, J.F., Carbonell, R., González-Lodeiro, F., Pérez-Estaún, A., Juhlin, C., Ayarza, P., Kashubin, A., Azor, A., Mart-ínez-Poyatos, D., Almodóvar, G.R., Pasdcual, E., Sáez, R., & Expósito, I. (2003), Crustal structure of the transpressional Variscan orogen of SW Iberia: SW Iberia deep seismic reflection profile (IBERSEIS), Tectonics, 22, 1062.

Simancas, J.F., Ayarza, P., Azor, A., Carbonell, R., Martínez Poyatos, D., Pérez-Estaún, A., González Lodeiro, F., (2013). A seismic geotraverse across the Iberian Variscides: orogenic shortening, collisional magmatism and orocline development. Tectonics 32, 417-432, 10.1002/tect.20035.

Sola, A.R., Pereira, M.F., Williams, I.S., Ribeiro, M.L., Neiva, A.M.R., Montero, P., Bea, F., and Zinger, T. (2008). New insights from U-Pb zircon dating of Early Ordovician magmatism on the northern Gondwana margin: The Urra Formation (SW Iberian Massif, Portugal). Tectonophysics 461, 114–129.

Tornos F. (2006). Environment of formation and styles of volcanogenic massive sulfides: The Iberian Pyrite Belt. Ore Geology Reviews 28: 259-307. https://www.sciencedirect.com/science/article/pii/S0169136805000296